LEHRSTUHL FÜR THERMOPROZESSTECHNIK
Lehrstuhlleiter:
Univ.Prof. Dipl.-Ing. Dr.techn. Harald Raupenstrauch
Montanuniversität Leoben
Franz-Josef-Strasse 18
A-8700 Leoben
www.unileoben.ac.at

Dissertation

Explosible Dust/Air Mixtures

Investigations on flame propagation under non atmospheric conditions

submitted to

Chair of Thermal Processing Technology

Submitted by:
Dipl.- Ing. Hannes Kern
0130935

Approved by:
Univ.Prof. Dipl.-Ing. Dr.techn. Harald Raupenstrauch
Univ.Prof. Dr.-Ing. Uli Barth

Leoben, 4.11.2013

EIDESSTATTLICHE ERKLÄRUNG

Ich erkläre an Eides statt, dass ich diese Arbeit selbstständig verfasst, andere als die angegebenen Quellen und Hilfsmittel nicht benutzt und mich auch sonst keiner unerlaubten Hilfsmittel bedient habe.

AFFIDAVIT

I declare in lieu of oath that I wrote this thesis and performed the associated research myself using exclusively resources cited in this volume.

_____ _____

Ort/Datum Unterschrift

Danksagung

Neben allen fachlichen Voraussetzungen erfordert das Verfassen einer Dissertationsschrift ein gewisses Maß an Selbstdisziplin. Doch selbst damit kann bestenfalls einen Teil dessen bewältigt werden, was für den erfolgreichen Abschluss dieses Studien- und Lebensabschnittes notwendig ist. Vor allem bedarf es vieler Menschen die einen einerseits unterstützen andererseits aber auch einfach dabei behilflich sind sein Ziel nicht aus den Augen zu verlieren. Nun hatte ich das große Glück mich auf zahlreiche solcher Menschen stützen zu können. Hierbei möchte ich zu allererst Professor Dr.-techn. Harald Raupenstrauch erwähnen, der mich nun doch schon einige Jahre begleitet und mir immer wieder die nötigen Freiräume für die Umsetzung meiner Ideen gelassen hat. Ohne ihn wäre es mir wohl nicht gelungen diese Arbeit zu verfassen. Gerade für die Umsetzung von Ideen und kreativen Gedanken braucht es auch ein persönliches Umfeld, das einem unterstützend zur Seite steht. Manchmal geht es aber auch nur darum aufzuzeigen, dass die eine oder andere fachliche oder persönliche Niederlage auch eine Chance sein kann. Dafür möchte ich meinen Freunden danken die mich nicht nur immer wieder auf andere Gedanken bringen sondern diese allzu oft auch mittragen. Mein besonderer Dank gilt allerdings meinen Eltern, welche die Grundlage dafür geschaffen haben, privat und beruflich jener Tätigkeit nach zu gehen, die mir auch persönlich viel Freude bereitet. Es sei gesagt, dass es gar nicht notwendig ist inhaltlich immer jedes Detail zu kennen wenn die Sache an sich positiv und fruchtbar ist.

Danke und Glück Auf!

Abstract:

In general, explosion hazards are a well-known risk in the process industries. However, the hazard of dust explosions is still underestimated in certain industrial areas. A clear understanding of the reaction mechanisms is crucial for the prediction of dust explosions. Research on dust explosion behaviour under non-atmospheric conditions leads to results allowing a more detailed investigation of influencing parameters on explosion reactions in general. For this thesis the influence of reduced pressure conditions as well as the influence of different inert gases on flame propagation has been studied. For this purpose, experimental devices to measure flame velocity were developed and experiments were carried out at different dust concentrations, at varying oxygen levels and at pressures down to 200 mbar. While flame velocity showed a linear decrease with decreasing oxygen concentrations, velocity at reduced pressure conditions reached its maximum below atmospheric conditions. The mechanisms of ignition were also of special interest with fundamental deviations from normal conditions observed.

Kurzfassung:

Explosionsgefahren sind in vielen industriellen Bereichen bereits seit Jahrzehnten bekannt. Die Gefahren von Staubexplosionen werden aber in manchen Industriezweigen immer noch unterschätzt. Kenntnis über die Reaktionsmechanismen und ein Verständnis der Zündvorgänge und Abläufe während einer Explosion sind Voraussetzung für eine Beschreibung von Staubexplosionen. Untersuchungen unter nicht atmosphärischen Bedingungen können den Einfluß verschiedener Parameter auch unter atmosphärischen Bedingungen deutlicher machen. In dieser Arbeit wurden vor allem die Auswirkungen von reduziertem Druck und verschiedenen Gaszusammensetzungen auf die Flammenfortpflanzung untersucht. Zur Ermittlung der Flammengeschwindigkeit wurden spezielle Versuchsapparaturen entwickelt und Versuche mit verschiedenen Sauerstoffkonzentrationen und bei Drücken von bis zu 200 mbar durchgeführt. Während die Reduktion des Sauerstoffgehaltes auch zu geringeren Flammengeschwindigkeiten führte, zeigten die Experimente bei reduzierten Druckbedingungen ein Geschwindigkeitsmaximum. Besonderes Interesse galt auch den Zündmechanismen, welche ebenfalls ein abweichendes Verhalten zu den Normalbedingungen zeigten.

Table of Contents

Acronyms and Abbreviations

BAM	Bundesanstalt für Materialforschung und Prüfung
BIA	Berufsgenossenschaftliches Institut für Arbeitssicherheit
DIN	Deutsches Institut für Normung
IE	Ignition Energy
LEL	Lower Explosion Limit
LOC	Limiting Oxygen Concentration
MIE	Minimum Ignition Energy
MIT	Minimum Ignition Temperature
NFPA	National Fire Protection Association
NIOSH	National Institute for Occupational Safety and Health
TPT	Chair of Thermal Processing Technology
UEL	Upper Explosion Limit
VDI	Verein Deutscher Ingenieure

List of figures

List of tables

1 Introduction

In general, explosion hazards are a well-known risk in the process industries. In contrast to gas explosions, the risk of an explosion occurring from combustible dusts is still underestimated in some industrial sectors. Dust explosions are historically tightly connected to mining and agriculture. For example firedamp explosions combining the characteristics of gas and dust explosions have been a known risk in the production and exploration of coal and other raw materials for hundreds of years. Many of these catastrophic events have led to improvements in safety regulation in the affected branch of industry. The explosion in the Farmingtion coal mine in 1968 (Figure 1) represents such a case.

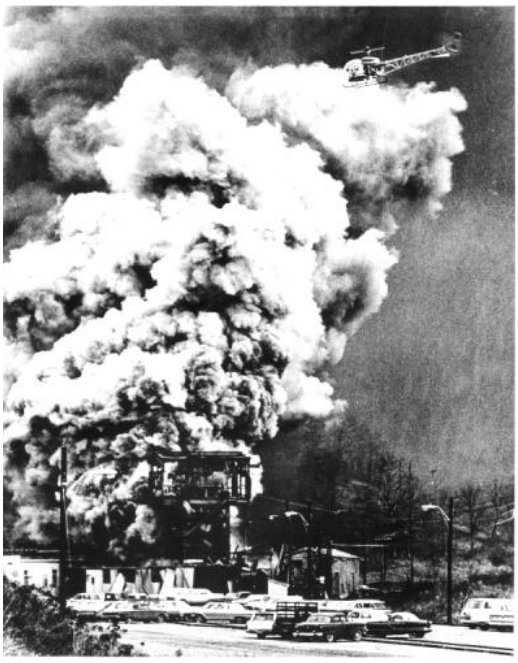

Figure 1: Explosion in the Farmington coal mine on November 20th 1968 [1]

As a consequence the Federal Coal Mine Health and Safety Act of 1969 [2] declared the following goal its primary purpose:

"…the first priority and concern of all in the coal mining

industry must be the health and safety

of its most precious resource--the miner."

As mentioned above, not only mining but also agricultural industries still suffer from catastrophic events. A recent example is the huge explosion at the Imperial Sugar Company in Georgia/USA in 2008 (Figure 2) leaving 14 dead and 36 injured [4].

Dust explosion prevention is therefore an important issue in health and safety regulation in most industrialised countries.

Figure 2: Dust explosion at the Imperial Sugar company on Feb.7th 2008, Georgia, USA [4]

The tight connection between dust explosion events and certain fields of industry creates a misleading picture of dust explosion hazards in the present industrial environment because new materials such as nano powders and newly-developed production processes create dust explosion hazards in areas that have not been affected by these problems before (Figure 3). The intensification of modern industrial processes leads to process conditions not differing from ambient conditions. Since dust explosion testing has mostly emerged the classical industrial fields traditionally connected to dust hazard, it lacks methods fit for the description and testing of dusts under deviating process conditions.

Figure 3: Aluminium dust explosion at Hayes Lemmerz Int. on Oct. 29th 2003, Huntington, USA [6]

Dust explosion research still faces fundamental problems in the explanation and evaluation of basic parameters of dust explosions, such as minimum ignition energy and temperature as well as those that define flame propagation like flame velocities. Much experimental and theoretical work has already been done but the sheer complexity of the problem still leaves many questions unanswered [3]. Dust explosion testing, for example, still relies on methods that are only able to determine explosion effects under very specific circumstances by sum parameters [5]. These safety-relevant parameters have been determined for a huge range of substances and are made available by different databases. Any new method used as basis for hazard analysis is compared to the present set of parameters. The deduction of physical or chemical mechanisms from such experiments is usually not possible. A more knowledge-based approach towards the fundamentals of combustion and ignition would be helpful in the description of dust explosions for example, in complex geometries by mathematical models. A clear understanding of the reaction mechanisms is also crucial for the prediction of dust explosions under non atmospheric conditions. In contrast, research on dust explosions behaviour under non atmospheric conditions leads to results that allow a more detailed investigation of the parameters influencing explosion reactions. The present thesis should contribute to the essentials of dust explosion processes under conditions that deviate from standard ambient conditions. The results gained from these investigations should also lead to a better understanding of dust explosions in general.

1.1 Fundamental preconditions for dust explosions

Due to the fact that the first severe dust explosions mostly occurred in coal mines or grain mills, dust explosion hazards are often mainly associated with mining or the processing of agricultural products. In modern industries combustible dusts are present in various fields of production. In every process in which fine combustible particles are present or produced, dust explosion hazards are risks that have to be considered.

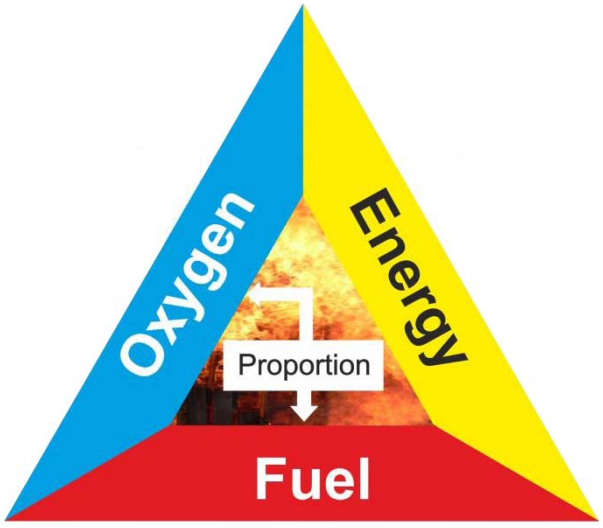

Figure 4: Explosion triangle

Figure 4 demonstrated the basic preconditions for the occurrence of fires and explosions. The three factors oxygen, ignition energy and fuel have to be present at the same time in order to cause continuous self-sustaining combustion. More important than for the development of fires, the right proportion between oxygen and fuel is an elementary factor for the ignition of explosive mixtures of gases with oxygen or dusts and oxygen.

In comparison to gas explosions the boundary conditions that influence the behaviour of the fuel are much more complex for combustible dusts. Conditions such as particle diameter and shape, dust composition, humidity and turbulence influence the development of dust explosions significantly. A lot of these influencing parameters have been scientifically investigated satisfactory, but present explosion testing devices only give results under certain limited conditions, and are heavily influenced by the testing procedures and devices themselves. The results of standardised testing methods considered as safety-relevant parameters that describe the explosion behaviour of different dusts under defined

experimental conditions. The direct translation of these parameters to actual process conditions is often impossible or inadmissible. Yet in spite of these problems, safety relevant parameters are vital for hazard analysis because of their comparability rather thean because of their quantitative values.

1.2 Safety relevant parameters

In terms of dust explosion testing, standard testing procedures are well-known and well established [7]. Besides the ignition behaviour of dust clouds, the determination of explosion effects is described in international standards. Most of these parameters are sum parameters through which detailed information on the combustion or ignition process itself cannot be determined.

A selection of the most important current safety-relevant parameters and the corresponding standard testing procedures are described below. These short descriptions should provide an overview of the present situation in dust explosion testing. The biggest problem concerning the application of safety-relevant parameters is that most of them are strongly influenced by the testing procedure itself. These parameters allow only a comparison of different substances under more or less defined conditions. The results obtained reveal deviations of several percent and can only be regarded as a hint concerning the behaviour of the mixture at conditions not matching standardised conditions.

1.2.1 Minimum Ignition energy

A demonstrated by the explosion triangle, ignition energy is one of the basic requirements for an explosion to occur. Regarding the fact that different chemical reactions require distinct activation energies, it can be assumed that the energy required to ignite an explosible mixture also largely depends on the fuel type if all other surrounding conditions are constant. For explosible dust/air mixtures, it is not only the chemical reaction of combustion that influences the required ignition energy but also physical conditions such as particle size and distribution, turbulence, thermal behaviour of the dust, humidity, etc.

Testing of the minimum ignition energy (MIE) is carried out by devices using electrical sparks of defined energy to ignite a dust cloud at its most reactive concentration. That concentration normally lies near the stoichiometric concentration of dust dispersed in air. Devices like these also allow the creation of more or less comparable turbulence conditions

by delaying ignition after the dispersion process. Spark duration can be influenced by the use of inductors and capacitors.

Figure 5 illustrates the development of a dust flame inside a MIKE 3 (Kuhner Safety) [8] testing device. The MIKE 3 testing device consists of a glass tube with a volume of about 1.1 l. The dust sample is dispersed by an air blast (50 ml) over a dispersion cone at the bottom of the device. The MIKE 3 apparatus is specially designed for explosible dust testing and provides ignition energies between 1 mJ and 1000 mJ.

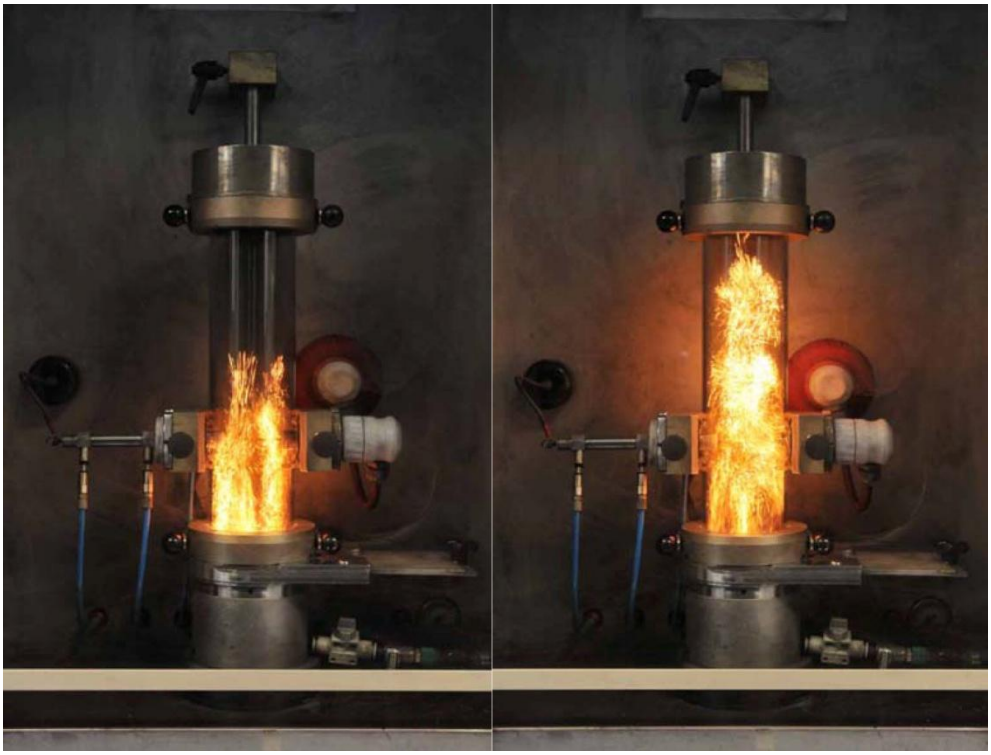

Figure 5: Flame development in a dust cloud after electrical spark ignition [9]

Several tests at different concentrations have to be carried out in order to be able to statistically ensure that no ignition can occur at defined spark energies.

1.2.2 Maximum explosion pressure and rate of pressure rise

The avoidance of an ignition source is one of the most effective strategies in explosion prevention but unfortunately not always possible. Therefore measures installed to mitigate the effects of an explosion are common. To allow proper design of such measures, the explosion behaviour itself has to be characterised. Besides a rapid rise of temperature, the most significant indicators for the severity of an explosion are the maximum explosion pressure (p_{max}) and maximum rate of pressure rise (dp/dt).

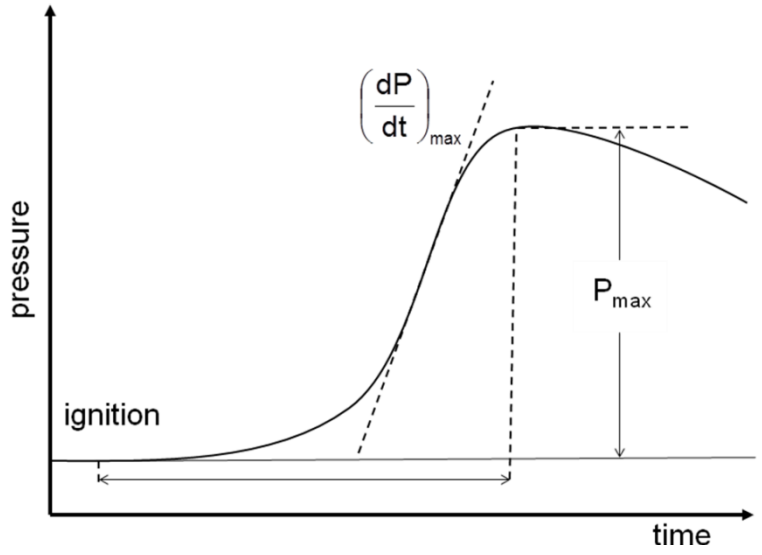

Figure 6: Pressure development during an explosion in a closed vessel

According to international standards, the standard testing apparatus for these parameters is a spherical device with a volume of 1 m³. Due to the big amount of sample material necessary and thus huge experimental efforts, the 1 m³ sphere did not seem practicable as a standard laboratory method. Studies of Bartknecht et. al. [10] have revealed that the course of an explosion and also the maximum explosion pressure strongly depend on the testing device itself. They showed that the volume of the testing apparatus and the ignition source have a strong influence on the results. Therefore, some kind of up-scaling factor had to be found to create a practicable solution with reliable results. In terms of volume dependence, the so-called “cube root law” was developed to determine a characteristic value for the rate of pressure rise, the K_{St}– value (Eq. 1-1).

$$\left(\frac{dp}{dt}\right)_{max} \cdot V^{\frac{1}{3}} = konst = K_{St} \qquad \textbf{(1-1)}$$

Bartknecht [10] also discovered that results from a 20 l spherical explosion chamber with chemical igniters of 10 kJ could be scaled up to the 1 m³ standard sphere with similar ignition energies. The 20 l sphere is easier to handle under laboratory conditions and is commonly used as standard testing device, although standards still refer to the 1 m³ apparatus.

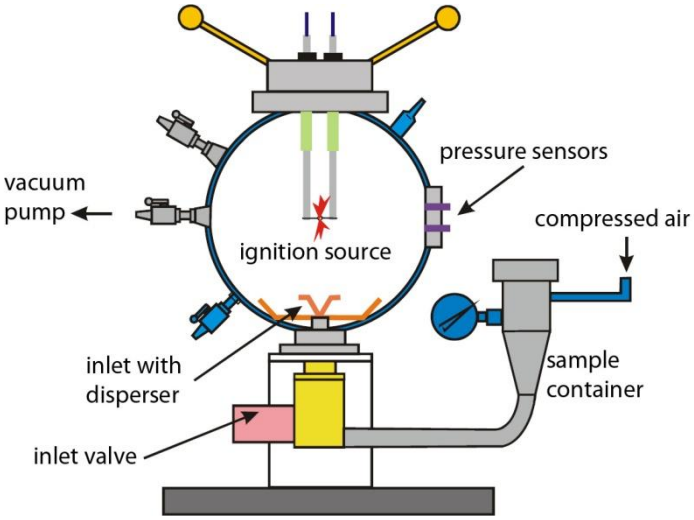

Figure 7: 20 l sphere for explosion testing [11]

The 20 l sphere (ÖNORM 14034-1) consists of a spherical double jacket steel corpus with a dust inlet system at the bottom and a cleaning hole with an integrated ignition system at the top. After evacuation of the sphere, the sample is brought into the system from a pressurised sample container over a fast opening valve and a dispersion system. The dispersion system should lead to a homogeneous dispersion of the dust sample inside the explosion chamber. Ignition can be conducted by electrical sparks but is in fact carried out by chemical igniters with defined ignition energy in standard procedures. To be able to create defined turbulence conditions, ignition starts after a short delay of 60 ms. Pressure sensors allow measurement of the maximum explosion pressure and the maximum rate of pressure rise after ignition [13].

The K_{St}- value as well as its counterpart K_G for combustible gases is mainly used for the classification of combustible dusts and for the design of different safety installations. Depending on the K_{St} value, combustible dusts are classified in three classes as provided in Table 1.

Table 1: K_{St} values of combustible dusts [10]

Dust explosion class	K_{St} [bar▪m/s]
ST 1	>0 - 200
ST 2	200 - 300
ST 3	> 300

The strong dependence on the testing conditions for the K_{St}- value shows that a comprehensive solution for the determination of safety-relevant parameters for combustible dust is still to be found. The new NFPA 68 Standard on explosion prevention by deflagration venting has recently replaced the K_G- value as the basis for the calculation of deflagration vents by the laminar burning velocity of combustible gases due to that problem.

1.2.3 Minimum ignition temperature of dust clouds

The minimum ignition temperature (MIT) of dust clouds is the lowest temperature of a hot surface able to ignite a dust cloud suspended in air. The MIT of dust clouds is measured in the so-called “BAM Oven” or a “Godbert Greenwald Oven”. Both devices mainly consist of a tempered oven where the dust suspended in air is ignited by the hot surface of the oven (Godbert Greenwald Oven) or a special concave plate (BAM Oven).

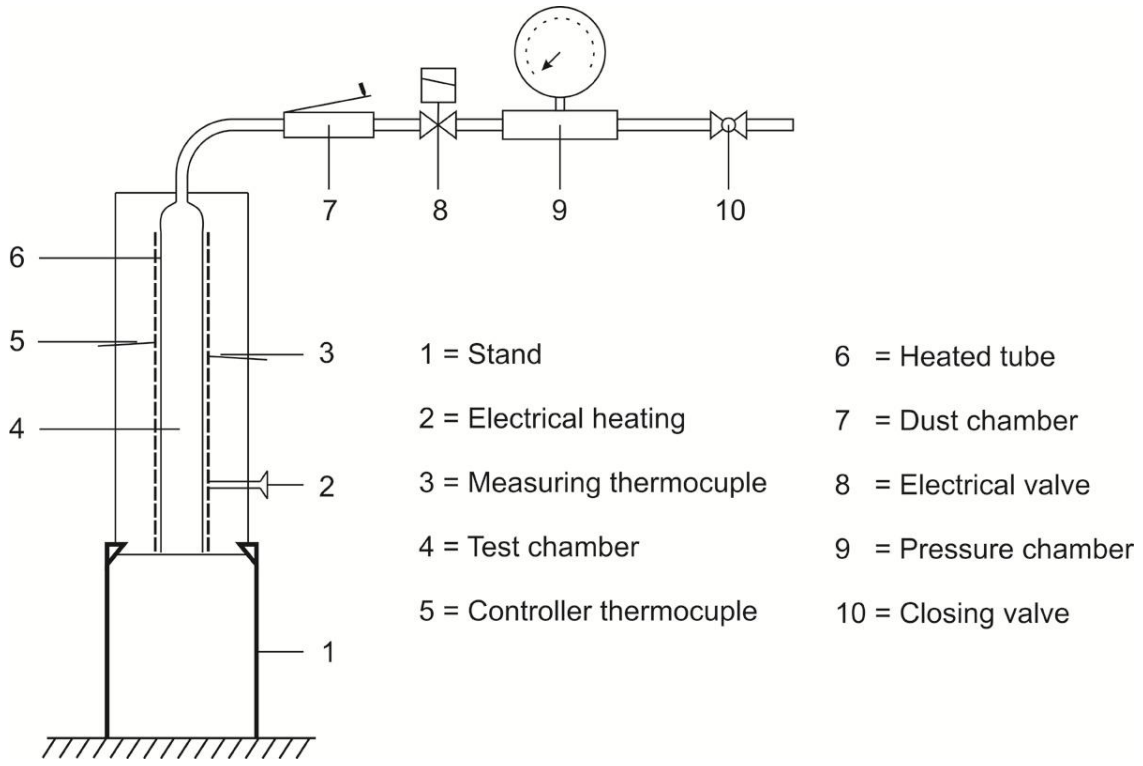

Figure 8: Godbert Greenwald Oven [15]

The values obtained by the two different experimental set-ups exhibit strong deviations. A variation of up to 80°C can be observed for specific dusts. The values from the BAM Oven are on average about 10 % lower than those from the Godbert Greenwald Oven [10]. This phenomenon proves that the experimental method heavily influences the results.

1.2.4 Explosion limits

A fundamental precondition for explosive combustion is the right proportion between oxygen and fuel. Explosions only occur within a certain range of fuel concentration that is also known as the explosive range. The explosive range is limited by a lower explosion limit (LEL) and an upper explosion limit. While mixtures of fuel and oxygen with fuel concentrations below the lower explosion limit can be considered as lean, mixtures with fuel concentrations above the upper explosion limit are too rich to be ignited. The explosion limits are substance-specific parameters and are linked to the combustion reaction itself. Within the explosion limits, combustion is more or less fuel-controlled. Burning velocity increases at concentrations close to the stoichiometric concentration for the combustion reaction. The stoichiometric concentration is also connected to a minimum of ignition energy and to a maximum of explosion severity. This explains why it is important to cover a wide range of concentrations during the experimental testing. Explosion limits are also linked to the physical properties (particle size, shape etc.) of the investigated dust. This is especially relevant in dust explosion testing.

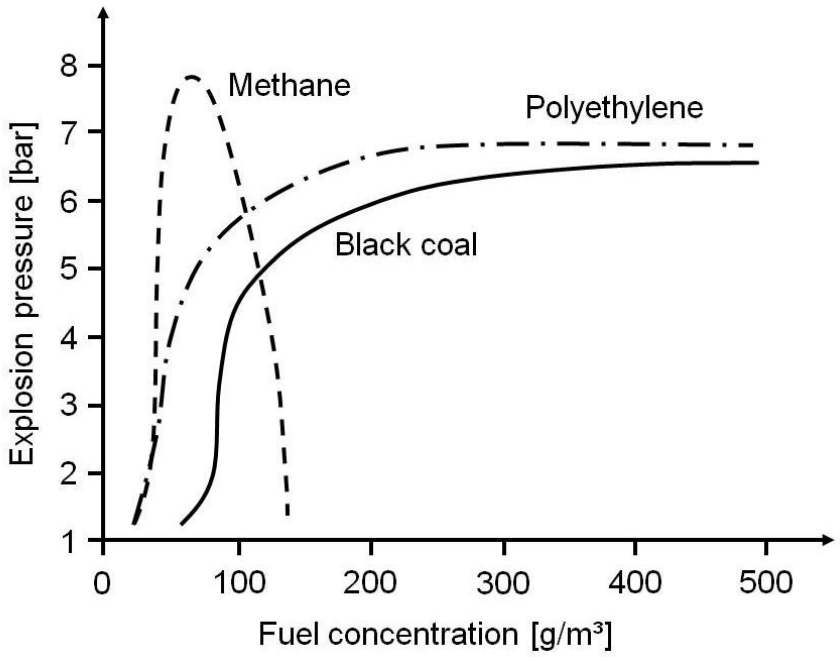

Figure 9: Relation between dust concentration and explosion pressure [16]

Combustible dusts often do not show a distinct upper explosion limit. Therefore, the upper explosion limit is not that important as a safety relevant parameter for preventive measures as it is for combustible gases. Figure 9 provides experimental results obtained by Bartknecht that allow the comparison of methane as combustible gas with two different combustible

dusts in terms of explosion limits. No defined upper explosion limit was found for the two dusts investigated within the concentration range of the experiments. Explosive behaviour can be found at concentrations of up to several kg/m³, which indicates reactivity also at very low burn-off rates.

Based on the definition of the lower explosion level as the limit for flame propagation due to a lack of fuel, Schönewald [17] discovered a relation to calculate the lower explosion limit of a combustible dust out of the higher heating value and parameters empirically found for different dust types (Eq. 1-2).

$$LEL = \frac{a}{HHV} - b \qquad \textbf{(1-2)}$$

The empirically determined parameters depend on different substance groups that have already been investigated. The parameters are available for powders used for coatings, technical dusts, fuel dusts and inorganic dusts (Table 2).

Table 2: Empirical parameters for the calculation of the LEL found by Schönewald

Coefficients	Coating powders	Technical dusts	Fuel dusts	Inorganic dusts
a [J/m³]	$1.235 \cdot 10^6$	$1.194 \cdot 10^6$	$1.390 \cdot 10^6$	$1.132 \cdot 10^6$
b [J/m³]	2.532	0.604	7.952	1.540

1.2.5 Limiting oxygen concentration

The limiting oxygen concentration (LOC) of combustible dusts is a basic parameter for the layout of safety measures based on inerting. It represents an oxygen concentration at which no ignition can occur even at very high ignition energies. While combustion behaviour around the explosive limits is fuel-controlled, combustion near the limiting oxygen concentration is oxygen-controlled. The limiting oxygen concentration must always be seen in context with inerting gas used to suppress the oxygen concentration. Gases with high specific heat capacities and high molecular weight exhibit better inerting effects than gases with comparatively low values for c_p. Most values are available for nitrogen inerting but also values for carbon dioxide or argon are known. Due to economic considerations, N_2 and CO_2 are most commonly used.

The experimental determination of the LOC in the 20 l sphere according to ÖNORM 14034-4 is the standard method but, requires extensive experimental work. Values for the maximum rate of pressure rise $(dp/dt)_{max}$ have to be determined at different oxygen concentrations. During lowering the oxygen concentration, $(dp/dt)_{max}$ shows linear decay. The limiting oxygen concentration is estimated by extrapolation of the values to an oxygen concentration where $(dp/dt)_{max}$ = 0 bar/s. This result is later on validated by further tests at the thus estimated oxygen concentration.

$$LOC = 1.8 \cdot \log(MIE') \frac{MIT + 273}{273} - 2.7 \cdot \log(E) + 12.8 \qquad \textbf{(1-3)}$$

Bartknecht [10] developed an empiric relation for the calculation of the LOC out of the minimum ignition temperature MIT, the minimum ignition energy at defined turbulence MIT' and the ignition energy IE (Eq. 1-3). Bartknechts relation allows only a rough estimation of the LOC, but it gives insight on the influencing factors of the limiting oxygen concentration.

Based on Schönewald's relation for the lower explosion limit, Krause [19] established a method for the determination of the limiting oxygen concentration by referring to a calculated fuel specific value σ_f that takes into account the chemical composition of the fuel with the focus on the mass fractions of carbon μ_C and hydrogen μ_H (Eq. 1-4).

$$\sigma_f = \upsilon_{O_2, C \rightarrow CO_2} \cdot \frac{\mu_C}{M_C} + \upsilon_{O_2, H \rightarrow H_2O} \cdot \frac{\mu_H}{M_H} - \frac{\mu_{O_2}}{M_{O_2}} \qquad \textbf{(1-4)}$$

Combined with Schönewald's relation, the fuel specific value can be calculated using the higher heating value HHV of the fuel and the empiric constants a and b used by Schönewald (Eq. 1-5).

$$\sigma_f = \frac{LOC \cdot \rho_{O_2}}{100 \cdot M_{O_2} \cdot \left(\frac{a}{HHV} - b \right)} \qquad \textbf{(1-5)}$$

After calculating the fuel specific parameter the limiting oxygen concentration is determined graphically by the use of Figure 10.

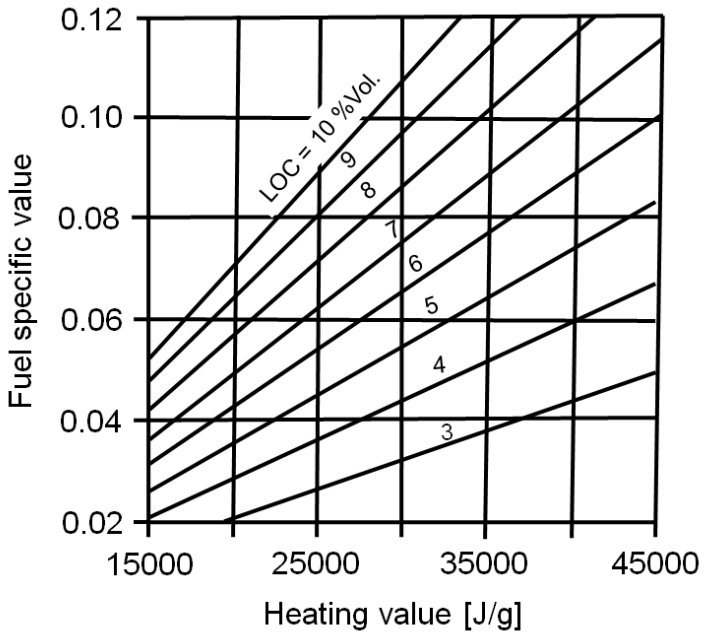

Figure 10: Diagram for the determination of the LOC by Krause [19]

The method described by Krause leads to a significant reduction of experimental effort for the determination of the LOC thanks to the use of standard parameters of fuel analysis. Krauses results for the LOC are on average lower than those obtained by experimental methods, but deviate less than the results gained using Bartknecht's equation.

1.3 Dust explosions in complex geometries

In contrast to the ideal conditions normally present in laboratory test facilities, dust explosions occurring during industrial accidents take place in complex geometries, often at non-ambient conditions. Large scale experiments have shown that the influencing parameters present at explosion incidents in complex geometries lead to effects deviating strongly from standard testing (Figure 11).

Figure 11: Large scale explosion experiment in a complex industrial system [20]

The description of explosions in complex geometries is vital to the planning of explosion mitigation systems such as pressure vents or explosion suppression systems. The simple fact that expensive large scale explosion testing is not feasible for every vessel or pipe system used in industry, demonstrates that dust explosion modeling and simulation are of special importance in risk evaluation and the planning of safety measures.

One of the challenges in dust explosion simulation is to be able to describe the explosion reaction based on chemical reactions or by experimental parameters that are representative for the combustion process itself. Current testing methods produce results that are highly influenced by the testing procedure themselves, which also influences the quality of the mathematical models. A more knowledge-based approach towards ignition and combustion as well as a better understanding of the combustion process would facilitate the prediction of explosion processes and improve the design of safety systems.

2 Fundamentals of ignition

Understanding the ignition process is a fundamental aspect in the investigation of ignition sources and the combustion process itself. In this chapter ignition mechanisms and influencing parameters on ignition will be discussed. The influence of oxygen concentration and material-specific parameters such as particle size on ignition will be of special interest [21]. Discussion of these influencing parameters is vital for the understanding of the combustion process under non atmospheric conditions.

2.1 **Mechanisms of ignition** [22], [23]

A large variety of ignition sources is able to trigger an explosion process. In dust explosion testing the use of chemical igniters and electrical sparks (due to experimental reproducibility) is common. In general, a distinction has to be made between the mechanisms of spark ignition and other ignition processes such as hot surface ignition. For investigations especially around the limits of ignition, electrical sparks are frequently used. Chemical igniters normally used in the 20 L apparatus provide far too much ignition energy and thus do not allow studying processes at the first steps of ignition. Electrical sparks can provide lower ignition energies and lower turbulence levels during ignition than chemical igniters [24]. Ignition is the starting point for further flame propagation and has to release enough energy to initiate self-sustaining combustion [22]. Different mechanisms are described for the processes during this initial stage of flame propagation. For combustible dusts, combustion and ignition are multi step reactions not only on the molecular level but also on a macro

scale. Processes like heating of the particle, pyrolysis or the evaporation of water are energy-consuming and thus the ignition energy required.

2.1.1 Ignition of combustible gases [22]

Because of their importance in the automotive industries, ignition processes are described comparetively well for combustible gases and vapours. Different theoretical models are known for the description of the ignition process itself. A good description for the mechanism of ignition is provided by Semenov's "Thermal Explosion Theory". This theory is based on the assumption that the heat production rate in chemical reactions features an exponential increase at rising temperatures whereas heat loss increases linear. Depending on the magnitude of the heat loss and heat release, different points of intersection will occur. In Figure 12, the temperature dependence of the heat production of three different exothermic reaction systems ($\dot{Q}_1 - \dot{Q}_3$) is illustrated.

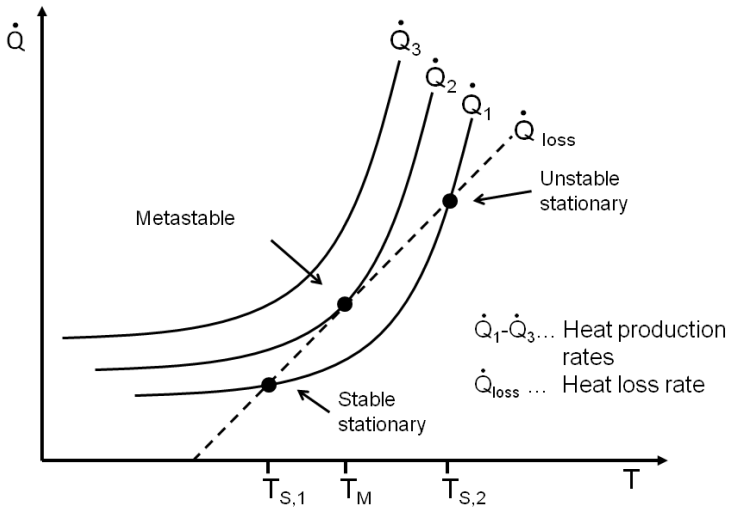

Figure 12: Temperature depencence of heat production and heat loss [22]

The dotted line represents the heat loss rate. Reaction $\dot{Q}_1$ has two points of intersection with the heat loss line. These points represent stationary reaction conditions with the difference that the point at temperature $T_{s,1}$ can be considered stable whereas the point at $T_{s,2}$ has to be considered stationary but unstable. At the stable point, a slight increase of temperature leads to higher heat generation which is opposed by an even higher heat loss rate. Therefore, reaction temperature decreases and the stable point of intersection is reached again. In terms of ignition this point represents an ignition source that cannot provide sufficient ignition energy to start the combustion process.

In contrast to the stable point, a slight increase of temperature in the unstable point ($T_{s,2}$) leads to a significant increase of the heat production rate. The amount of heat produced by the reaction can not be dissipated by heat transfer processes. Temperature therefore continues to rise, eventually leading to ignition. The metastable point at temperature T_M of curve $\dot{Q}_2$ represents a condition where an infinitesimal increase of the reaction temperature leads to ignition. This point represents a highly reactive fuel/oxidant mixture that only needs very low energy input to in order to be ignited. Curve $\dot{Q}_3$ represents the extreme condition of a reactive system that ignites at any given temperature.

For gas and vapour reactions the ignition behaviour is mainly determined by the chemistry of the combustion reaction, the turbulence level and the specific heat capacity of the reactive mixture [25]. Ignition energy is needed to heat inert components of the reactive mixture and to heat up the reactive system itself. As described above, the basic idea for the description of the ignition process is a simple heat balance. The energy brought into a defined ignition volume must be higher than any heat losses by convection, radiation or conduction in order to be able to raise temperature in an initial flame kernel. Figure 13 describes the relation between distance from the centre of the flame kernel and heat production as well as heat loss.

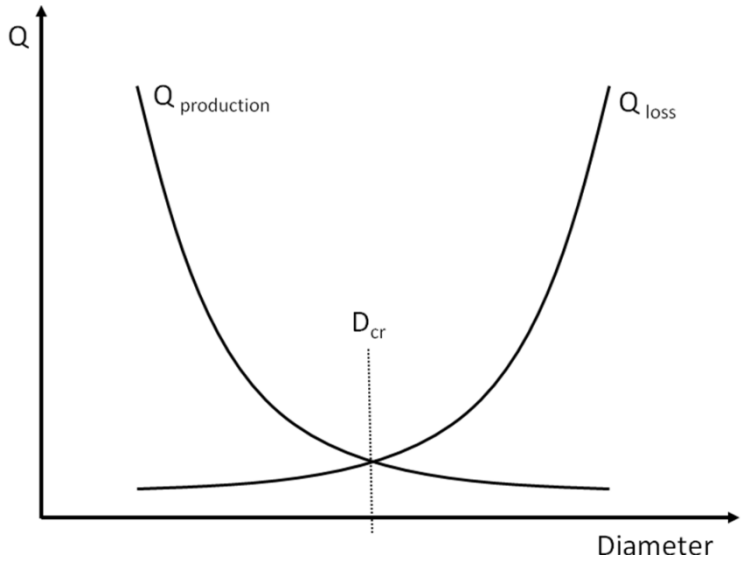

Figure 13: Heat balance in the flame kernel [26]

At the postulated initial flame volume, the heat of combustion ($Q_{production}$) is proportional to the diameter of the flame ball and heat loss (Q_{loss}) increases in proportion to the volume. The point of intersection between these two processes represents the critical flame ball diameter that needs to be reached for ignition. Heat transfer out of the initial ignition volume is present

by convection (initial turbulence), conduction (diffusion processes) or radiation. Convective heat transfer based on turbulence has an especially big influence on the ignition process. Knowledge about the turbulence conditions at the start of the ignition process is therefore vital for the description of ignition.

The critical ignition volume is strongly linked to a critical or minimum heat release rate that has to be initiated by an external ignition source. Based on these considerations Proust [27] developed a simple relation for the estimation of the minimum ignition energy (MIE) of combustible gas/air mixtures. Proust describes the relation between MIE, the thermal conductivity of the gas mixture λ, the critical diameter of the ignition kernel D_{cr} and the adiabatic flame temperature T_{ad} as follows (2-1)

$$MIE \approx \lambda \cdot D_{cr} \cdot T_{ad} \qquad \textbf{(2-1)}$$

The diameter of any given spherical flame ball is related to the laminar flame velocity S_u and the burning time t_B (2-2)

$$D \approx S_u \cdot t_B \qquad \textbf{(2-2)}$$

Combining these equations the minimum ignition energy can be expressed by the following set of equations (2-3, 2-4, 2-5).

$$MIE = \int \lambda \cdot D_{cr} \cdot T_{ad} \cdot dt \qquad \textbf{(2-3)}$$

$$MIE = \int \frac{\lambda \cdot D_{cr} \cdot T_{ad}}{S_u} \cdot dD \qquad \textbf{(2-4)}$$

$$MIE = \lambda \cdot \frac{D_{cr}^2 \cdot T_{ad}}{2 \cdot S_u} \qquad \textbf{(2-5)}$$

The equation described yields good results for explosible gas/air mixtures. For combustible dusts, the measurement of the critical flame ball diameter and also the laminar flame velocity is quite complicated due to the influence of turbulence on ignition and combustion created by the ignition source.

2.1.2 Ignition of combustible dusts

The ignition of combustible gases mainly depends on the chemistry and mechanism of the combustion reaction as well as on heat transfer phenomena in the gas phase. For combustible dusts, processes such as the heating of the particle or pyrolysis (organic dusts) have to be considered. The ignition and combustion of dusts is, besides the chemical combustion reaction, a multi step reaction also on the macro scale. Depending on the material, different regimes of combustion can be defined. Van der Wel [28] describes three main reaction mechanisms for combustible dusts. He distinguishes between the following reaction types:

- Reactions on a solid or liquid surface, forming gaseous products
- Reactions on a solid or liquid surface, forming solid or liquid products
- Reactions in the gas phase, forming solid, liquid or gaseous products

The first two reaction regimes are limited by the transport of oxygen or combustion products into or out of the particle. The third type is dominated by the formation of combustible vapours or gases which provide fuel for the gas phase reaction. Yet, looking at the large variety of combustible dusts, most combustion reactions are a combination of these regimes. Lycopodium (spores of clubmoss), for example, contains significant amounts of oil (40-50 %) embedded in a porous solid structure. This results in a primary gas phase reaction followed by the combustion of the solid material.

According to the Semenov theory, a combustible dust needs to release a certain amount of energy during ignition to enable the chain reactions of combustion. It can be observed that, neglecting physical conditions such as particle size or shape, the minimum ignition energy largely depends on the substance itself and is therefore a parameter specific to the combustible mixture. In terms of energy release, the standard enthalpy of combustion is a substance specific parameter. In combustion technology calorific values are normally determined in bomb calorimeters that provide the so-called higher and lower heating values (HHV, LHV) indicating the amount of energy released during combustion. Higher heating values are tabulated for a large number of materials. Heating value and minimum ignition energy seem to define the reactivity of a material. Materials with high heating values can show high as well as low minimum ignition energies, which is also true for materials with low

heating values. However, dusts with high heating values and low minimum ignition energies can generally be considered as highly reactive (e.g. aluminium).

For combustible gases or vapours, the minimum ignition energy in mixture with air normally lies below 1 mJ. The presence of inert components influences the required ignition energy drastically. Inert gases, for example, are considered as heat sinks during ignition and combustion. Other heat sinks such as inert solid particles act similarly. This suggests that for solid combustible particles a considerable amount of the ignition energy is needed to heat the combustible particle itself. Combustible dusts with particle diameters in the area of around 63 µm (standard median value for dust explosion testing) exhibit minimum ignition energies that lie significantly higher than 1 mJ. To describe the influence of particle size on ignition behaviour, Kalkert [29] postulated the following relation between particle size and minimum ignition energy (Eq. 2-6).

$$MIE = (4 \cdot \pi \cdot \kappa)^{3/2} \cdot \rho \cdot c \cdot [\frac{\ln 2}{12} \cdot \frac{\rho_s \cdot c_s}{\lambda}] \cdot T_{Fl} \cdot d^3 \qquad (2\text{-}6)$$

κ [-]	Ratio of specific heats
ρ [kg/m³]	Gas density
c [J/kg·K]	Spec. heat capacity oft the gas phase
ρ_s [kg/m³]	Density of the particle
c_s [J/kg·K]	Spec. heat capacity oft the particle
T_{Fl} [K]	Flame temperature
D [m]	Particle diameter

The relation presented by Kalkert suits a variety of combustible dusts but also underlies certain restrictions. The main conclusion is that particle size has significant influence on the minimum ignition energy. Nevertheless, the entire process of ignition is still not fully understood. On the one hand, the heating behaviour of the gas atmosphere in the ignition kernel is a major factor to be considered. On the other hand, heat transfer into the particle, thermal conduction processes within the particle, pyrolysis or vaporisation are energy-consuming steps during ignition that have to be taken in account as well.

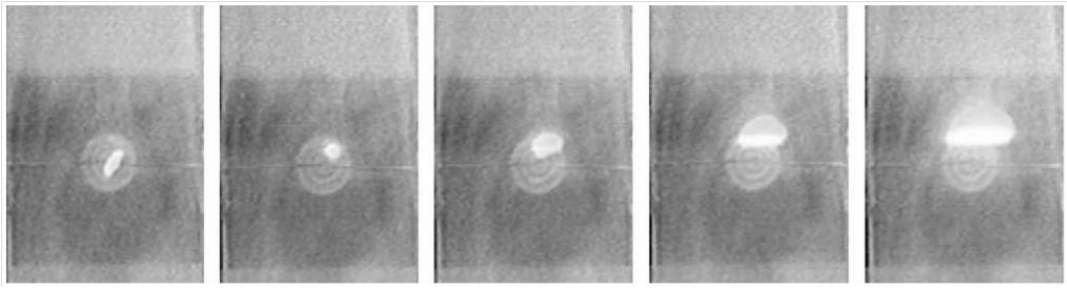

Figure 14: Developement of the flame kernel after igntion [26]

It is vital for the description of ignition mechanisms to be able to quantify the amount of energy needed for all steps of the ignition process. The mechanism of gas expansion and the influence of turbulence after spark ignition, are not completely understood. Considering the flame kernel approach, a distinct amount of dust particles has to be present inside the initial volume to supply enough energy for the start of the combustion reaction.

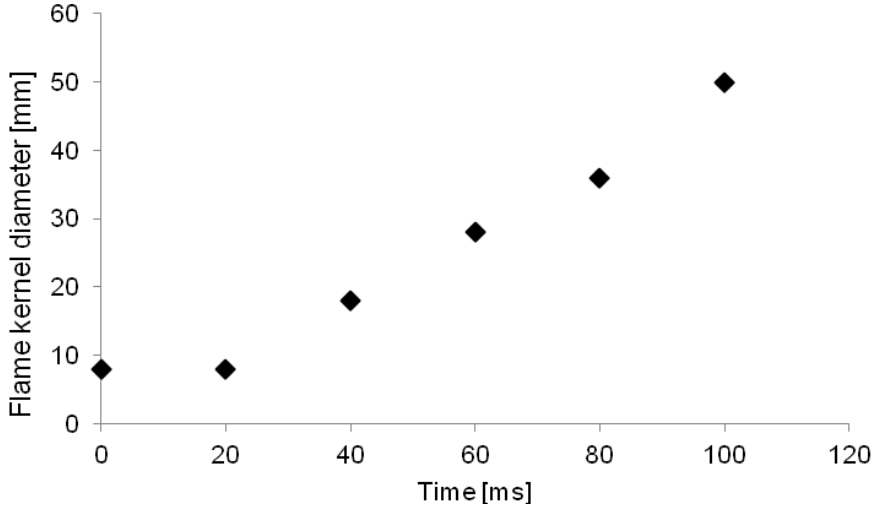

Figure 15: Flame growth after spark ignition in a starch/air mixture, measured by Proust [26]

Proust et al. measured the development of the flame kernel after ignition and found that for maize starch the flame kernel during spark ignition showed a constant diameter of around 7 mm in the first 20 ms. After 20 ms the flame ball grew linear. Regarding the ignition kernel, only limited data is available for other substances.

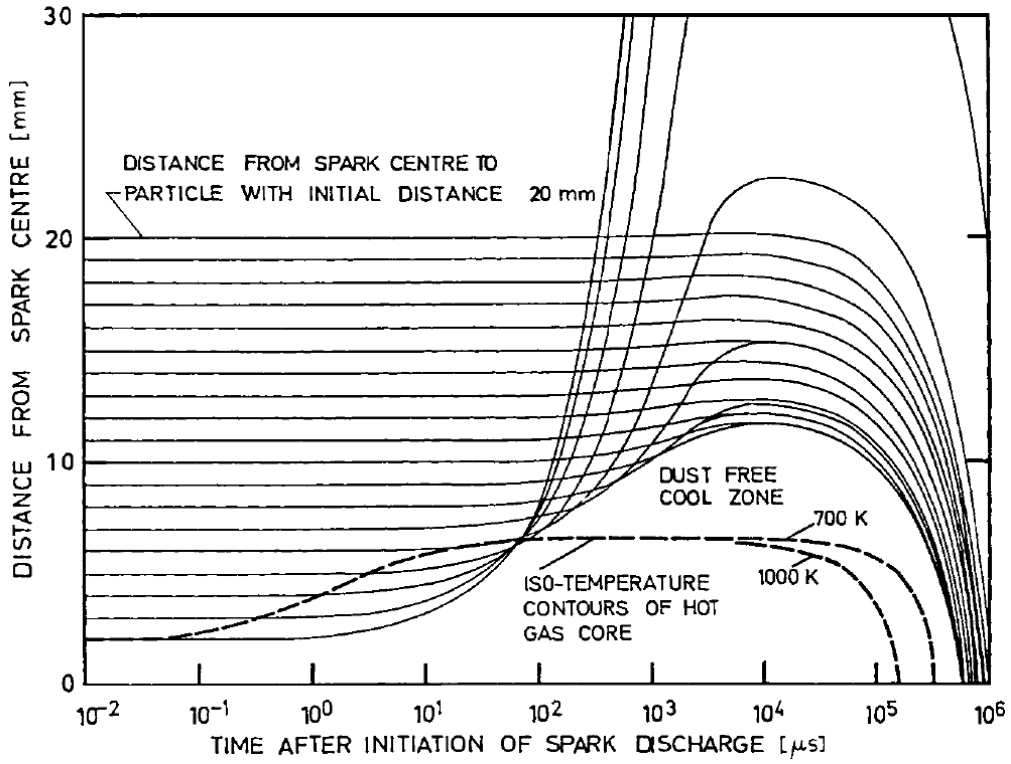

Figure 16: Theoretical prediction of the positions of lycopodium particles after spark discharge by Enstad [30]

For the development of the flame kernel, effects such as buoyancy of the hot gases formed during ignition have to be considered as well. Particles situated in the gap between the electrodes may be dragged away by the hot gas kernel, thus forming a particle front with a higher concentration than the one predominant in the bulk. Enstad [30] calculated the positions of lycopodium particles and the radius of the hot gas kernel after a spark discharge (1.5 J). The calculated kernel reaches a temperature of 1000 K at approximately 10 ms (Figure 16). The ignition energy used for Enstads calculations is significantly higher than necessary to ignite lycopodium air mixtures. At around 5 mJ, the minimum ignition energy of lycopodium is three orders of magnitude lower. Therefore, the effects of buoyancy are less pronounced and they do not influence the initial stage of ignition as strongly as higher ignition energies do.

2.2 Inert gases

As described in chapter 2.1, ignition is influenced by various heat transfer processes. For dust explosions, the dust particle itself (size, specific surface etc.) is, besides the gas atmosphere inside the ignition kernel, a main factor to be considered. With the exception of metal dust explosions, which mainly show a solid phase reaction, all other dust explosions are dominated by gas phase reactions of pyrolysis gases or a vaporized substance. The initiation of the gas phase reaction only demands a comparably low amount of energy. The amount of energy necessary to start the reaction increases as the oxidant concentration decreases, due to reaction kinetics and the influence of inert gases that substitute the oxidant. The activation energy of the combustion reaction will, for example, increase with lower oxygen concentrations.

Table 3: LOC values measured by Siwek in a 1m³ apparatus [10]

Inert gas	N_2	CO_2
Dust type	LOC [Vol.%]	LOC [Vol.%]
Lycopodium	11.0	15.0
HDPE	11.5	15.0
Coal	14.0	17.0
Pea flour	15.5	17.0

The presence of inert gases supports this effect by acting as a heat sink. Due to the different thermal characteristics of different inert gases, the limiting oxygen concentration is an inert gas specific value. For example Siwek et al. [31] demonstrated that carbon dioxide acts as a better inert gas than nitrogen (in comparison) (Table 3). Based on the LOC values measured at different concentrations of selected inert gases, Siwek developed a simple empiric relation for the conversion of LOC values obtained by nitrogen and carbon dioxide inerting (Eq. 2-7).

$$LOC_{CO_2} = 1.36 \cdot LOC_{N_2} \qquad \textbf{(2-7)}$$

Subsequent research revealed the values measured by Siwek as systematically too high [32] for both inert gases. Still, the relation allows good general comparison of the values obtained by different inert gases.

3 Fundamentals of flame propagation

As described in the previous chapters a stable fuel/air flame develops after ignition. In contrast to flame propagation through gas/air mixtures, flames of combustible dusts burn by multi-step physical and chemical processes. In the description of the burning process, considerations must not be limited to the chemical reactions of the combustion process itself the physical conditions of the dust (particle size and composition, porosity etc.) strongly influence the reaction as well.

In dust explosion testing, the measurement of flame velocity provides a more detailed insight on the combustion process than the record of pressure/time development measured in the 1 m³ or the 20 L sphere, which represents a more basic approach in terms of explosion modeling. This chapter presents a principal overview on flame propagation through dust/air mixtures. In addition, selected testing assemblies for the determination of the laminar flame velocity of dust/air flames are discussed.

3.1 Laminar flame velocity

When discussing flame propagation two phenomena have to be distinguished: the term “laminar flame velocity” on the one hand and the actual, observed flame velocity on the other hand.

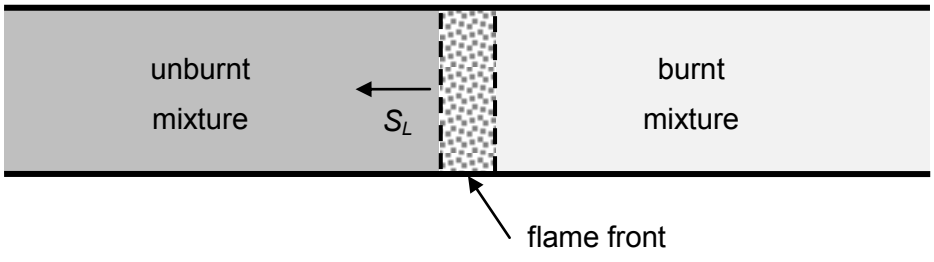

Figure 17: Laminar flame propagation in a fuel/air mixture

Concerning the combustion of a gas/air mixture, the ongoing process can be divided in three main zones as shown in Figure 17. The flame front is the distinguished area between the burnt and the unburnt fuel/oxidant mixture where the process of combustion or burning takes place [33]. The speed of the flame front travelling through a steady, homogeneous dispersed unburnt mixture is called laminar flame velocity S_L.

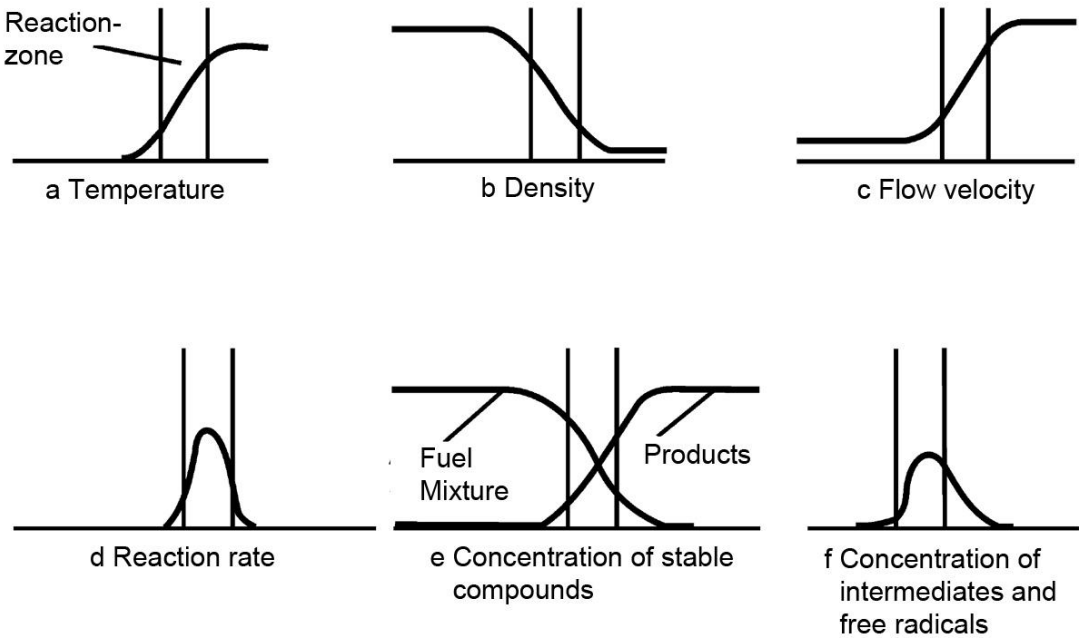

Figure 18: Development of different properties of a combustible mixture during combustion [34]

The laminar flame velocity is linked to different properties of the fuel/oxidant mixtures shown in Figure 18. As the maximum rate of temperature increase is reached within the combustion zone, the density of the mixture drops and the flow velocity increases (Figure 18 a-c). In the reaction zone, the reaction rate exhibits a maximum whereby also the concentration of intermediates reaches the highest level. However, their maximum is shifted towards the product side of the combustion zone due to kinetic effects (Figure 18 d-f). Flame thickness [35] is therefore strongly connected to the reaction rate combining the macro and micro kinetics of the combustion reaction.

Measurement of the laminar flame velocity is quite difficult under experimental conditions. Influencing parameters such as geometry, pressure, temperature or flow patterns (laminar or turbulent) have to be considered. Therefore, measuring the actual flame velocity in a defined experimental setup is more common. The flame velocity is easier to detect but influenced by the parameters mentioned above. Flame velocity is often measured by burners with steady

flames, in tube reactors or autoclaves. Tube reactors are especially common in dust explosion research and will be discussed in the following chapters.

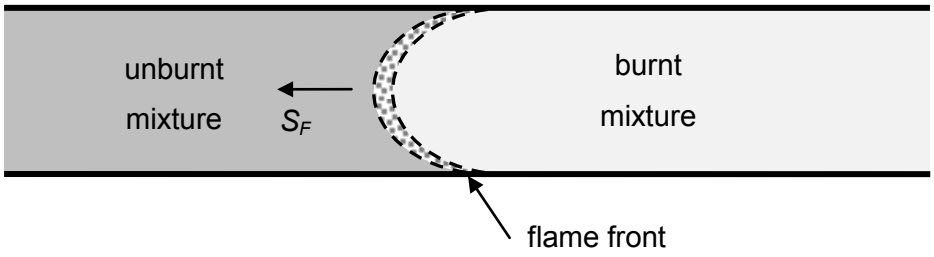

Figure 19: Flame shape in tubular reactors

With reference to the flame shape forming during experiments in such combustion tubes, a different picture compared to the ideal steady circular and flat combustion zone can be observed. Wall effects and turbulence created by the travelling flame itself lead to flame shapes that exhibit more or less parabolic shape. The shape of the combustion zone leads to a larger combustion area and a stretched flame. Andrews and Bradley described an approach for the determination of the laminar flame velocity (S_L) in gas/air mixtures by the following relation (Eq. 3-1):

$$S_L = \frac{A'}{A_F} \cdot \left(S_F - u\right) \qquad \textbf{(3-1)}$$

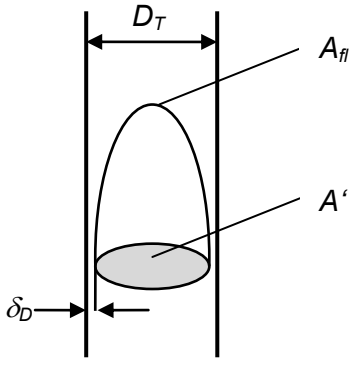

A_{fl}… surface of the flame cone

A‘… cross section covered by the flame cone

D_T…diameter of the combustion tube

δ_D… distance between flame and tube wall

Figure 20: Parameters for the calculation of the laminar flame velocity according to Andrews and Bradley [36]

The actual flame velocity (S_F) measured is corrected by the relation between the surface of the flame cone (A_F) and the cross section covered by the flame (A'), taking into account also the velocity of the gas flow (u) possibly present under non stationary conditions. A' differs from the tube diameter (D_T) by the boundary layer δ_D. According to Andrews and Bradley [36], the relation can be used for $S_F > S_L$. The measured flame velocity S_F exceeds the gas velocity u. Krause et al. [15] also used this relation for the calculation of flame velocity in dust/air mixtures in tube reactors.

3.2 Mechanism of flame propagation in lycopodium/air mixtures

Contrary to flame propagation in gas/air mixtures, flame development in dust/air mixtures strongly depends on the physical parameters of the fuel. Particle size and size distribution, chemical composition, moisture, porosity and various other factors influence burning behaviour.

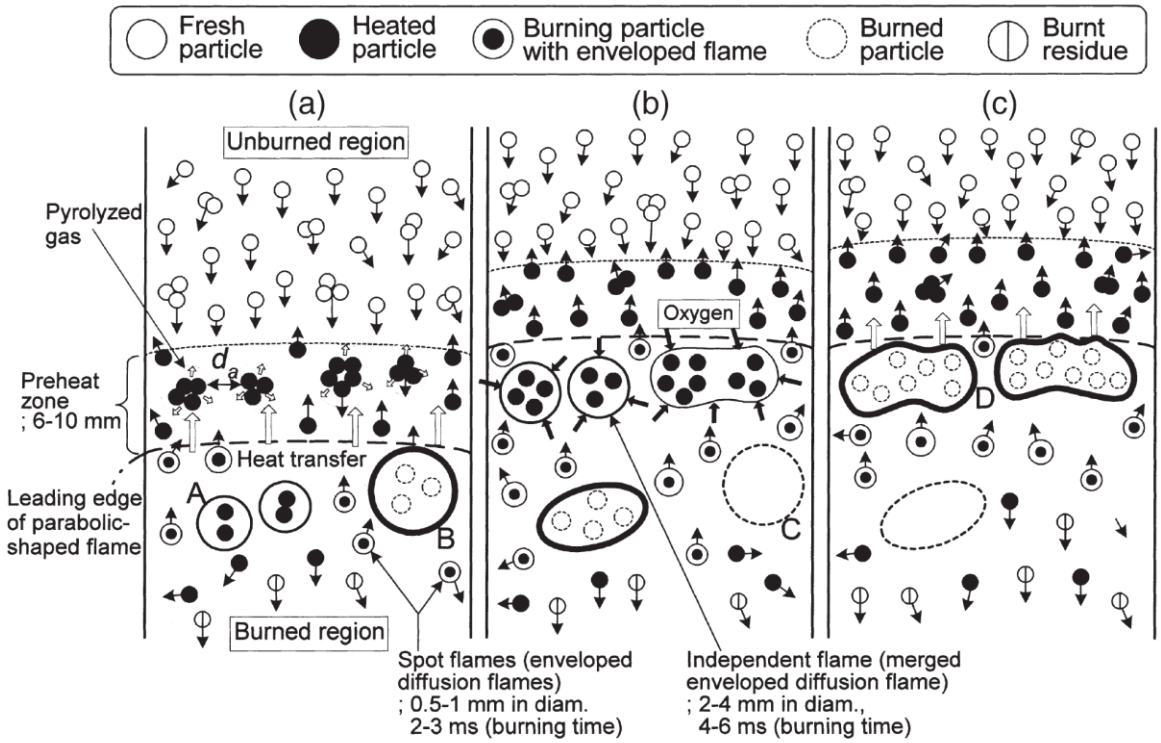

Figure 21: Mechanism of flame propagation in lycopodium/air mixtures by Han et al. [37]

A mechanism of laminar flame propagation through lycopodium/air mixtures in vertical ducts is described by Han et al. and shown in Figure 21. The flame develops different zones that exhibit flow patterns and particle concentrations that are slightly different from

homogeneous dust/air mixtures. Fresh particles move downwards due to gravitation and enter a preheat zone in front of the leading flame edge. Due to flow patterns in front of the leading flame edge, the particle movement downward stops and the particle moves upwards ahead of the leading flame edge. During its residence time in the preheat zone, pyrolysis takes place and the particle reaches its ignition temperature of around 425 - 460 °C [38]. The velocity of the flame front is higher than the upward moving velocity of the preheated particles in front of the leading flame edge. Particles heated over their ignition temperature sustain the flame front but leave the leading flame edge still burning. These burning particles form spot flames behind the leading flame edge.

Han et. al. also describe the formation of agglomerates formed by the particles. At lower dust concentrations, the leading flame edge is mostly sustained by single particles or smaller agglomerates that are heated significantly faster than bigger agglomerates of particles. The bigger agglomerates form independent flames behind the leading flame edge due to inferior heat transfer (A-C in Figure 21a,b). At higher dust concentrations an increase of burning velocity can be observed. The distance between the spot flames in the leading flame decreases, the spot flames eventually merge into a continuous flame front. The decreased distance between the particles leads to better heat transfer and higher burning temperatures (D in Figure 21c).

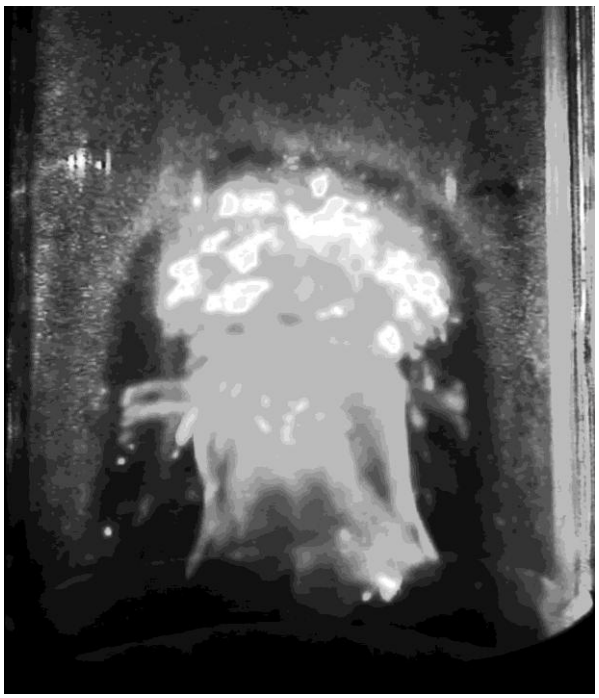

Figure 22: Flame propagation through a lycopodium/air mixture (100 g/m³)

Figure 22 shows a flame propagating through a lycopodium/air mixture of around 100 g/m³ in a vertical tube with a diameter of 140 mm. In front of the flame a homogeneous dust mixture is present. The different zones of combustion described by Han et. al. are clearly visible. The preheat zone has a thickness of around 8-10 mm. Particles are pushed away by the leading flame edge which leads to a slight increase of dust concentration ahead of the preheat zone. Near the leading flame edge single spot flames are visible in the preheat zone. Bigger agglomerates are building up behind the leading flame front and form independent flames. Single spot flames can still be seen up to around 100 mm behind the leading flame front. The picture was taken using a 2 mm slice of green laser light (532 nm) that illuminates the dust particles in a 90° angle to the camera perspective. An optical filter only allowing light from 520 nm to 560 nm to pass was used.

3.3 Experimental determination of flame velocities

The experimental investigation of dust/air flames is rather difficult because of the fact that homogeneous dust/air mixtures with low turbulence levels are comparatively hard to realise. Any kind of mixing procedure that creates undefined turbulence levels strongly influences the results of the experiments. Different experimental approaches to determine the flame velocity of dust/air flames are known.

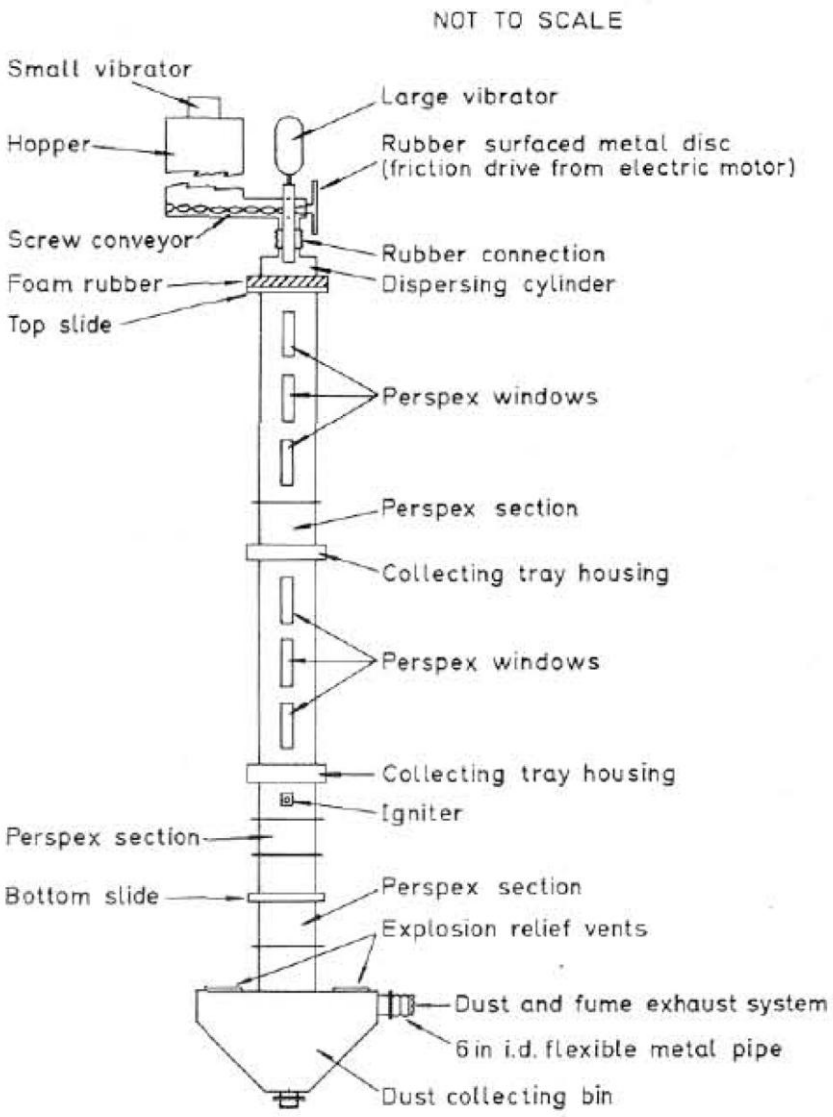

Figure 23: Experimental setup for the determination of the laminar flame velocity by Palmer and Tonkin [39]

A device used by Palmer and Tonkin [39] uses a screw conveyor with a vibrating dispersion device to feed the dust into a tubular combustion chamber. The advantage of this device is that the feed system on top of the combustion tube creates a very low turbulence

level at the point of ignition and the dust brought into the system disperses homogeneously over the cross section of the tube during settling. A big disadvantage of this system is that it is more or less closed on the bottom end. This leads to a pressure increase behind the flame front due to the expanding combustion products. To minimize the problem of flame acceleration due to expanding off gases Han et al. designed a testing device with a sliding bottom section that allows the expanding combustion products to be released to ambient pressure (Figure 24).

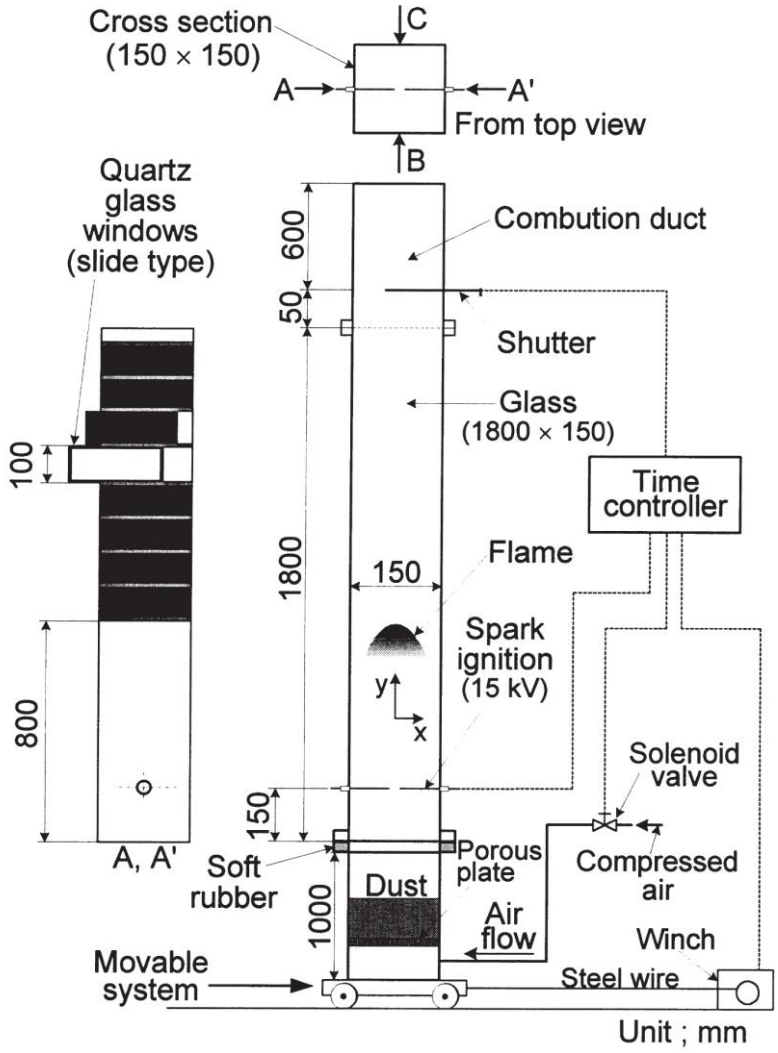

Figure 24: Apparatus for the measurement of laminar flame propagation by Han et al. [37][40]

The bottom section in Han's setting is also used for dust dispersion by a fluidized bed providing an upward gas flow and moved before ignition. Han et al. used optical systems and the measurement of the ionization potential for the determination of the flame velocity. Figure 25 provides the values measured by Han. The laminar flame velocity shows a maximum of

0.5 m/s at around 180 g/m³. At lower concentrations the flame speed drops rapidly towards the lower explosion limit. The decrease of the laminar flame speed at higher dust concentrations is less intense. Interestingly, the stoichiometric dust concentration of a lycopodium/air mixture lies at around 100 - 120 g/m³ [41], which leads to the conclusion that the combustion process in the reaction zone of the flame is incomplete.

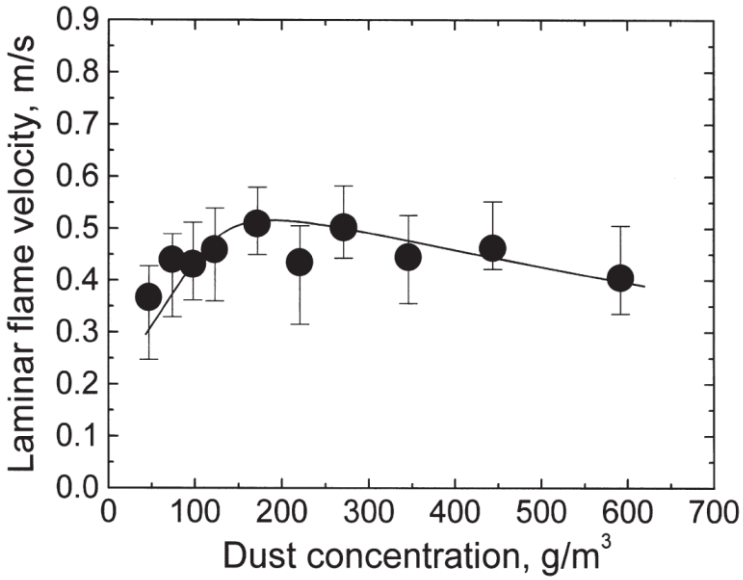

Figure 25: Laminar flame velocities of lycopodium/air mixtures measured by Han et al. [37]

A comparable approach for the determination of the laminar flame velocity was chosen by Krause et al. [15]. Krause et al. used a porous sinter plate to disperse a certain amount of dust and to create a defined dust concentration in transparent tubes of different diameters. A continuous and defined upward air flow was created inside the tube. The turbulence conditions were thus determined by the gas flow rate. During the experiments the bottom end of the tube remained closed. An optical system was used for the measurement of the flame speed. Due to the fact that a constant gas stream was provided through the bottom section the flame velocity measured must be corrected to get the laminar flame velocity S_L.

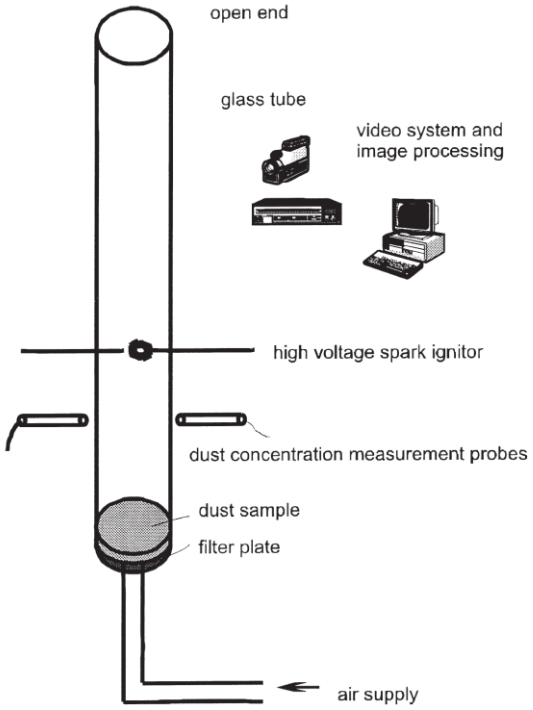

Figure 26: Combustion tube used for investigations on flame velocity by Krause et al. [15]

Krause et al. used Andrews and Bradley's relation (3-1) for the determination of the actual laminar flame velocity.

Table 4: Laminar flame velocities measured by Krause [15]

dust type	dust conc. [g/m³]	gas flow [m/s]	S_L [m/s]
Tube diameter = 60mm			
Lycopodium	200	0.39	0.28
Maize Starch	100	0.34	0.26
Wheat flour	120	0.34	0.23
Tube diameter =100mm			
Lycopodium	205	0.19	0.50
Maize Starch	375	0.30	0.40
Wheat flour	260	0.28	0.30

Krause et al. as well as Han et al. found the maximum laminar burning velocity for lycopodium at around 0.5 m/s, depending, as can be seen from Krause's data, on the tube diameter. Proust [26] found laminar flame velocities of corn starch/air from 0.15 m/s up to 0.23 m/s at concentrations of around 180 g/m³, which is considerably lower than the values found for lycopodium. Based on the assumption that the effect of turbulence must neither be neglected on the micro scale of the combustion reaction, Skjold has developed a method to calculate the laminar flame velocity out of the maximum rate of pressure rise obtained from experiments in the 20 l Siwek chamber. He calculated the laminar flame speed on the basis of the turbulent flame velocity. For corn starch at a concentration of around 140 g/m³, Skjold calculated a laminar flame speed of $9.0 \cdot 10^{-2}$ m/s, which is significantly lower than the experimental values by Proust. The data used by Skjold [41] to calculate the laminar flame speed were measured using also a significantly weaker ignition source than normally used in explosion testing. Skjold used a 6 J electrical spark discharge for his experiments. Such lower ignition energy creates lower initial turbulence than the normal 10 kJ chemical igniters used in dust explosion testing.

4 Experimental method

For further experimental investigations a setup has been developed on the basis of the different apparatuses described in literature [15] [26] [39] and on the considerations expressed in the previous chapters. The main goal was to find a setup that could be adapted to different experimental requirements without major changes. On the one hand a reduction of experimental effort had to be assured. On the other hand, high comparability of the results measured under different atmospheric conditions was desired. The focus of the investigation was laid on the ability to create homogeneous dust clouds in different air/inert gas mixtures and under reduced pressure conditions. In contrast the influence of higher temperatures on flame propagation was not within the scope of this work. For investigations on the principles of flame propagation, lycopodium was chosen as the test substance. As an organic substance with very narrow particle size distribution and high specific surface, lycopodium exhibits good characteristics for further investigations.

4.1 Basic experimental setup

In the development of dust explosions, turbulence is a key factor in addition to the specific characteristics of the dust itself. Therefore, an experimental setup had to be found that allowed the creation of a homogeneous dust cloud on the one hand and low turbulence conditions on the other hand. Apparatuses described by Krause et al. are able to provide a good particle distribution by using a constant gas flow through a sinter plate under constant but comparatively high turbulence conditions. Other apparatuses use dust feed systems at the top of the testing device, which requires accepting an inferior particle distribution and the

disadvantage of not being able to investigate dusts that tend to strongly agglomerate. Pre-tests showed that the dispersion of lycopodium in air could be realized quite easily. Therefore, a top feed arrangement for testing seemed adequate, especially in terms of low turbulence levels. Various dust concentrations are achievable with proper dust feeding systems. A top feed system also meets the requirements for investigations under reduced pressure conditions because no gas stream is required for dust dispersion.

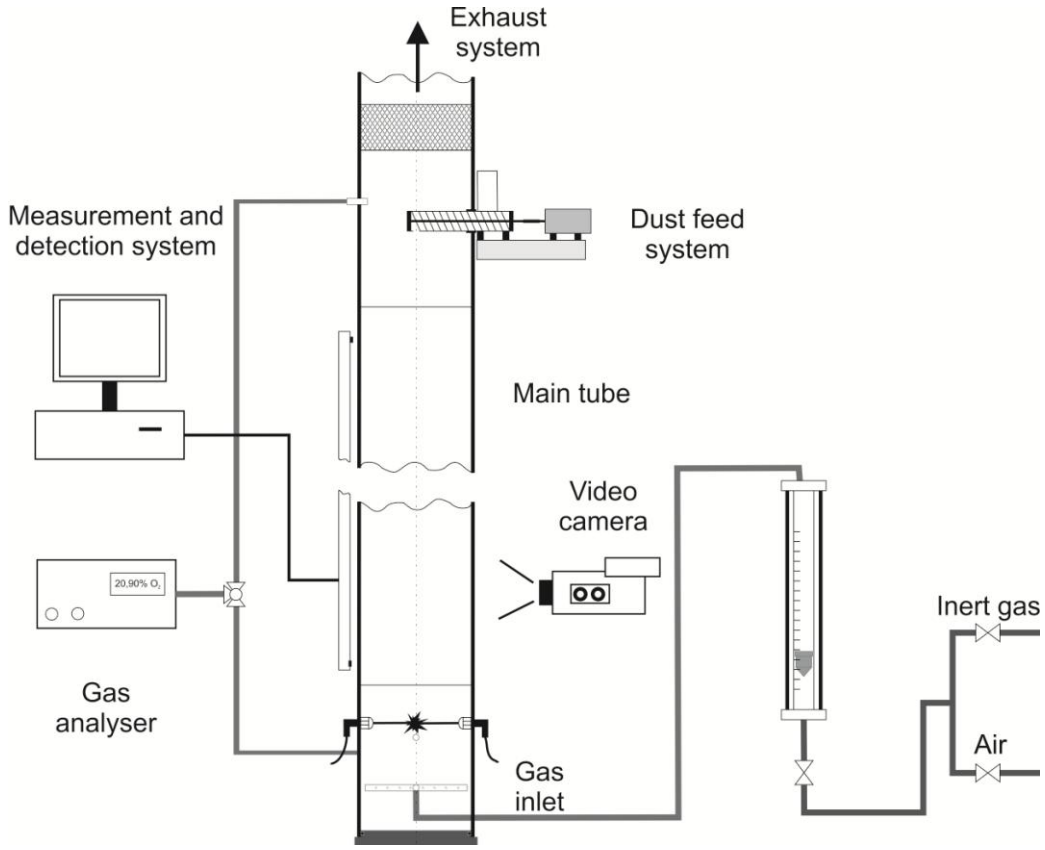

Figure 27: General assembly of a measuring device for flame propagation under presence of different inert gases

Experiments in closed vessels often do not allow the visual observation of flame propagation and explosion development. For investigations of flame development, optical systems allowing the determination of flame propagation as well as flame geometry are obligatory. Explosion tests carried out in a tubular testing apparatus with at least one opening allow design pressures around atmospheric conditions. For further experiments a main explosion tube made of Plexiglas® was chosen. A tube with an inner diameter of 140 mm and a wall thickness of 5 mm fulfilled the requirements for experiments at atmospheric as well as below atmospheric pressure conditions. The main parts of the experimental assembly

are discussed in detail below. Basically the apparatus consists of a bottom section that houses a gas inlet system and the spark ignition system, the main combustion tube and a top section with the dust feeding device and the gas outlet. Measurement and detection is conducted using an optical system with photodiodes and a video camera for the measurement of the flame shape.

In general, three different arrangements were used for the experiments. Figure 27 demonstrates the assembly used for investigations under presence of different inert gases. The device has a closed bottom end and is connected to an exhaust system on the top end.

Considering that an offgas pressure builds up behind the flame front ant thus leads to flame acceleration and inaccurate results in terms of laminar flame propagation, a setup with an open bottom end was tested to avoid this effect. This apparatus is shown in Figure 28.

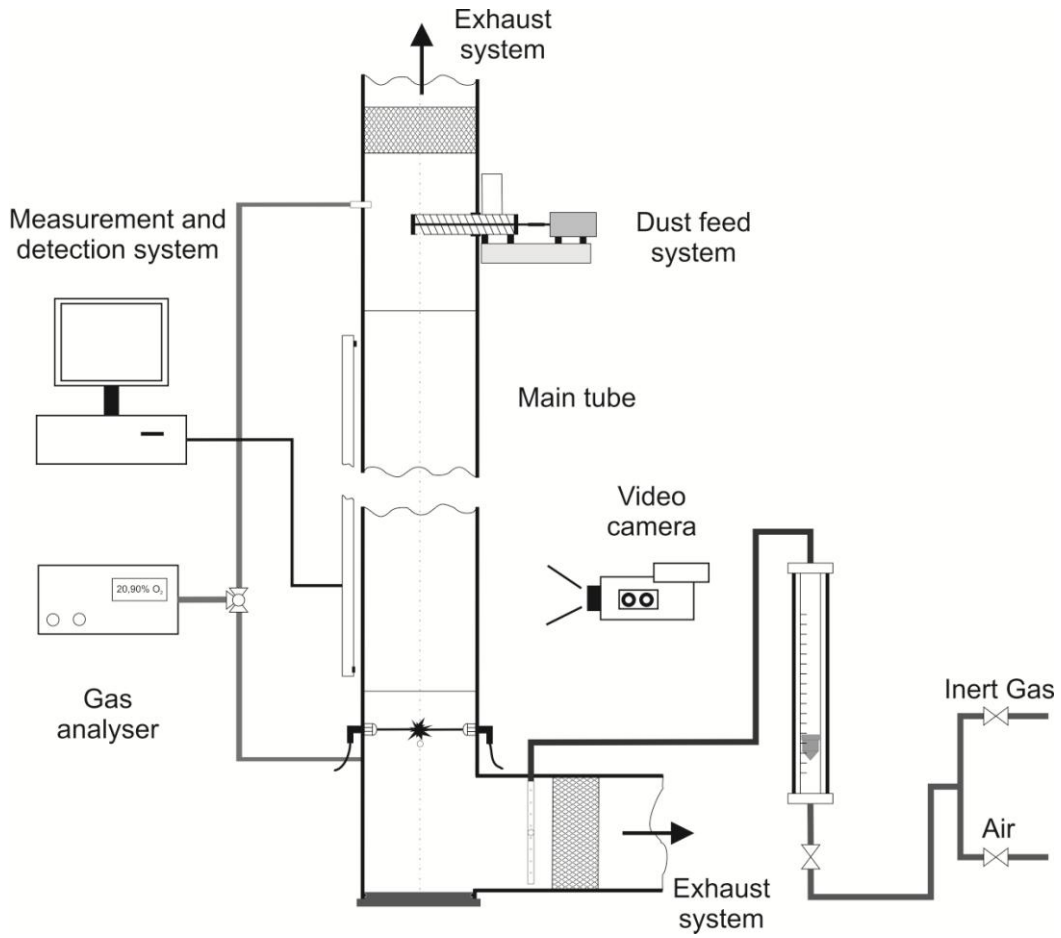

Figure 28: Experimental setup with open bottom end

This assembly had the disadvantage of a stack effect building up within the tube due to the connection to the exhaust system of the lab. To minimise this effect, a check valve was

added to the system to provide an undefined flow pattern inside the combustion tube. In the experimental phase the results obtained from this setup exhibited great variations [42]. Further research therefore concentrated on a closed bottom version of the combustion section. However, at least some useful results regarding laminar flame propagation could be gained also with the open version.

Experiments with pressure levels below atmospheric conditions required a completely sealed combustion section. The top section and the bottom section of the system were reconstructed and adapted according to the experimental requirements. Figure 29 shows the apparatus with the vacuum system and the re-designed top section.

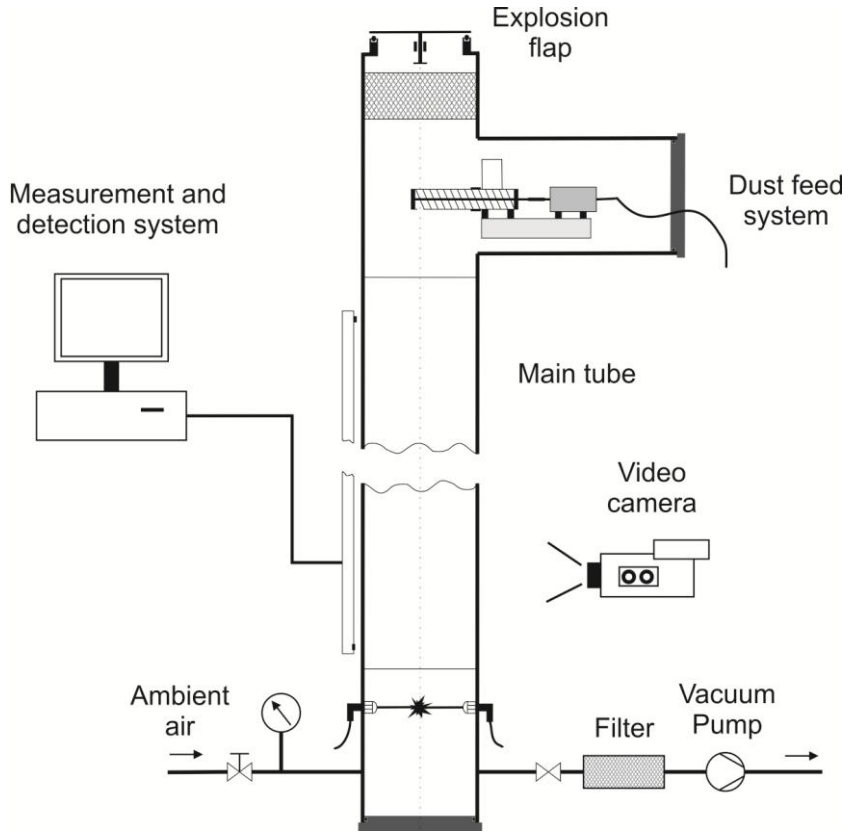

Figure 29: Testing assembly for experiments below atmospheric pressure

The vacuum pump used for the creation of the proper pressure conditions allowed a minimum absolute pressure of around 90 mbar. Due to Bartknecht's findings that an ignition below 20 mbar is not likely and the fact that the spark igniter used provided considerably low ignition energies, the pump characteristics proved to be satisfactory.

4.2 Safety considerations

Dealing with dust explosion that could create massive damage to persons and equipment experimental safety was a key issue during the experiments. Main considerations have been:

- control of flame spread
- pressure design
- relief systems for uncontrolled pressure build up
- fire protection

After a critical safety analysis, several modifications were made to the apparatus: flame arresters to keep the dust flame from spreading outside the combustion section and a pressure relief system to prevent the apparatus from uncontrolled overpressures.

4.2.1 Flame arresters

Flame arresters are frequently used in gas explosion protection but not very common in the field of dust explosions. Key parameter in the construction of flame arresters is the maximum experimental safe gap (MESG). The MESG is the minimum width of a gap where under defined experimental conditions no flame propagation is observable.

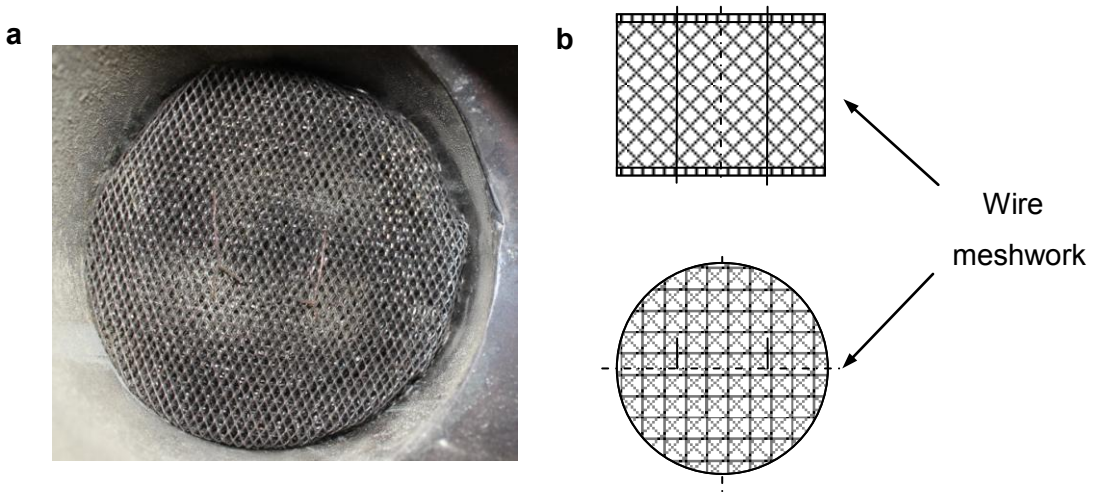

Figure 30: Flame arrester [43]

Flame arresters a shown in Figure 30 are constructed from wire meshwork or rolled undulated metal strips. All free cross sections of the arrester have to be below the MESG. In terms of dust explosion protection, this is problematic because of dust deposits. For the

current experimental setup the flame arrester proved a proper solution to prevent the flame from spreading outside the combustion tube thanks to periodical cleaning. The steel wire meshwork used had a height of 50 mm and covered the whole cross section of the combustion tube. For experiments with an open bottom end, two flame arresters were used, one at the top and one on the bottom of the tube.

4.2.2 Explosion flap

The construction of an apparatus for experiments under reduced pressure conditions proved rather challenging because a setup had to be found with a completely sealed combustion section to prevent the occurrence of any significant overpressure during the experiments.

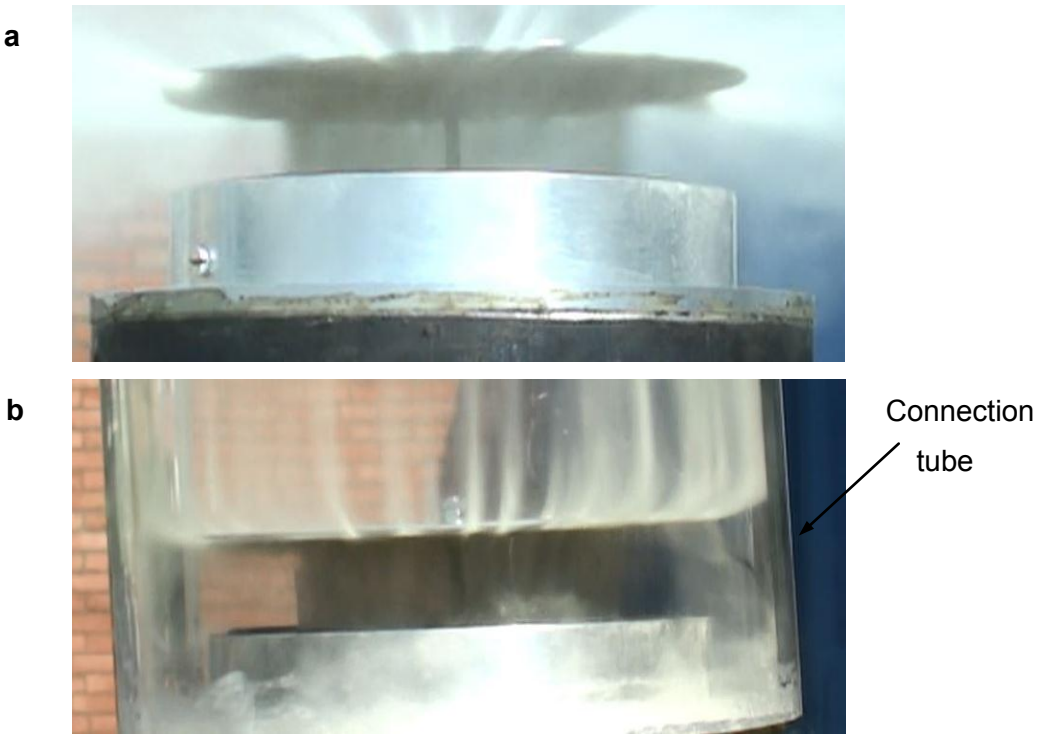

Figure 31: Testing of the explosion flap without (a) and with (b) connection to an off gas system [43]

Figure 31 demonstrates the explosion flap during testing with a dust concentration of around 200 g/m³. First, the device was tested without connection to an off gas system. After a successful test it was connected to a venting system with a transparent tube to allow visual inspection of the flap before and after experiments.

4.3 Dust cloud generation

Basically, the dust feed system is arranged as presented in Figure 32. A conveyor screw transports the lycopodium to the drop-off point in the centre of the combustion tube. The feed is controlled by a variable power supply that allows the generation of different dust concentrations inside the tube. The conveyor screw is placed before the flame arrester described above to prevent the flame from travelling into the exhaust system. Figure 32 shows the assembly that was chosen for the measurements with different inert gases. For experiments under lower pressure conditions, the conveyor screw was housed in order to be able to properly evacuate the whole setup.

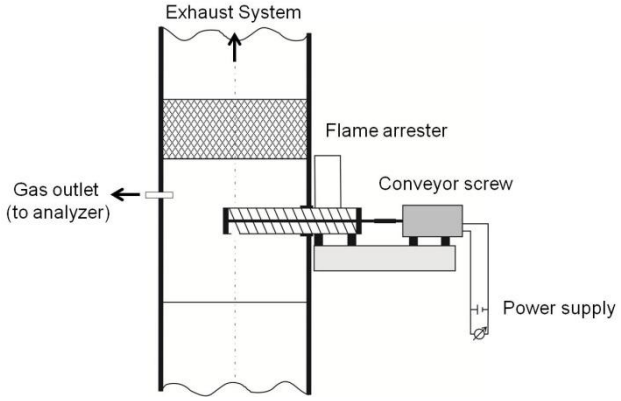

Figure 32: Top section of the experimental device for use under ambient pressure

For the generation of the dust cloud inside the tube, two different screw conveyors were used in order to be able to cover a wide range of possible dust concentrations. The first screw conveyor allowed feed rates from 0,1 g/s to 3,0 g/s but exhibited very unsteady conveyance at low rotation speeds. To enable steady conditions also at very low dust concentrations (<100 g/m³), a second conveyor screw was constructed, which allowed dust feed rates from 0,01 g/s to 0,1 g/s. It could be visually observed that at around 30-40 cm below the drop-off point the dust was totally dispersed over the whole profile of the tube. Results from CFD simulations provided the same value [44]. The calculations also showed that a stable dust concentration could be reached inside the tube after about 15-20 seconds. This value was verified by two concentration sensors at 100 mm and 500 mm above the ignition point. In further experimental work, the dust cloud was ignited after 20 seconds of dust feeding. In the first feeding experiments, the tube exhibited strong electrostatic effects. Large amounts of the lycopodium introduced by the conveyor screw stuck to the wall, thus influencing the dust concentration inside the tube. To mitigate electrostatic effects, the inner side of the tube was treated with an anti-electrostatic spray normally used in electronics. The

spray is based on ionic liquids which exhibit a very low vapour pressure and build up a conductive layer on the surface. The spray proved very effective and after treatment electrostatic effects could only be observed to a minor extent. Due to the chemical characteristics of the liquid, a contribution to the combustion process was not deemed very likely.

4.4 Dust concentration measurement

Proper measurement of the dust concentration inside the combustion tube was a basic requirement for all further research. Different methods were discussed during the development of the testing device. Optical sensors are commonly used in dust concentration measurement and also seemed applicable to the testing device, especially considering the fact, that the measurement of the flame speed was planned to be conducted by optical sensors.

Two lasers (532 nm, 1 mW) were installed at 100mm and 500mm above the ignition point in order to be able to measure the concentration of the dust cloud on the one hand and a possible deviation of the concentration inside the tube on the other hand. The lasers were installed outside the tube opposite two photodiodes used for flame velocity measurement.

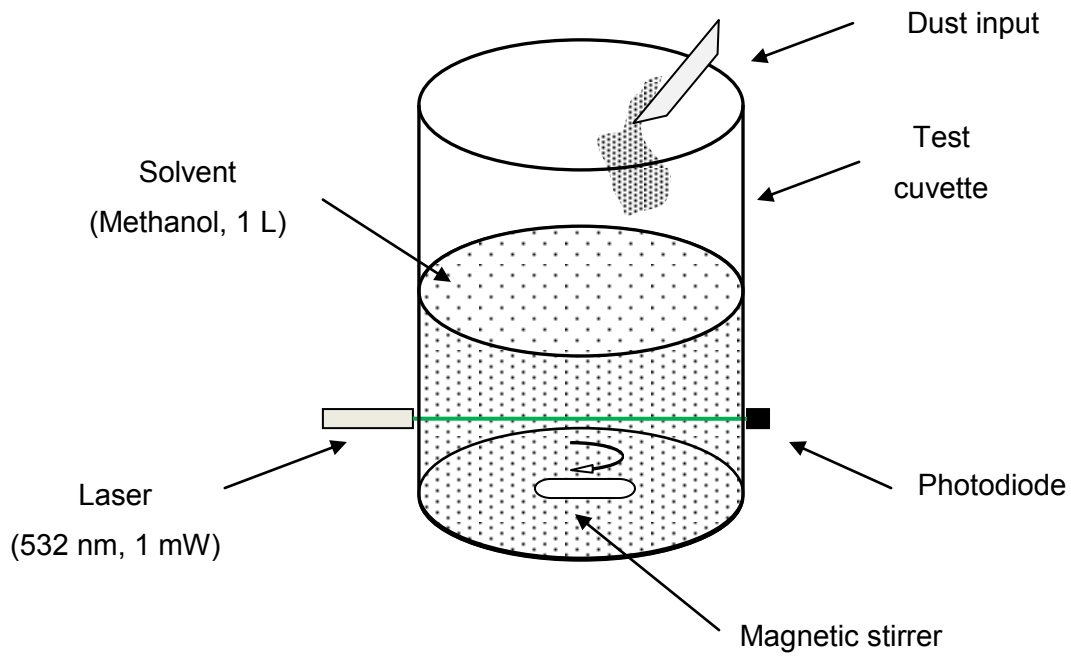

Figure 33: Setup for the calibration of the concentration measurement system

The calibration of sensors with dusts dispersed in air requires a lot of experimental effort and still might fail to prevent large deviations due to incomplete dispersion. Therefore, it was decided to use a liquid solvent which allowed homogeneous dispersion of lycopodium in a defined volume. The solvent had to exhibit low surface tension and be non-polar enough to allow the lycopodium particles, which contain considerably high amounts of natural oil, to be dispersed. A high transmissivity for the laser light was also necessary. Scheid [45] used methanol for the calibration of the dust sensors. The lasers used by Scheid emitted laser light with a wavelength of 645 nm. At 532 nm Methanol shows a lower transmissivity but allows a sufficient signal level for calibration. The calibration setup is described in Figure 33.

The calibration of the lasers was carried out using a 300 mm long test cuvette similar to the combustion tube used for the experiments on flame propagation. Exactly 1 liter of the solvent was filled into the cuvette. A magnetic stirrer was used to disperse the dust inside the cuvette before the measurement was carried out. During calibration the magnetic stirrer was turned off. Different dust concentrations were realised by adding certain amounts of lycopodium to the solvent. The transmissivity T was calculated by the following relation (Eq. 4-1):

$$T = \frac{I}{I_0} \qquad \textbf{(4-1)}$$

The variable I_0 represents the signal of the photodiode without dust present in the cuvette. The signal is only weakened by the present methanol. The signal measured is indicated by I. For calibration purposes, dust concentrations from 50 g/m³, 100 g/m³, 150 g/m³, 200 g/m³, 300 g/m³ and 500 g/m³ were created. The transmissivity values measured were later used to calibrate the dust feed system. For the calibration of the dust feed system the laser diodes were placed along the combustion tube, different feed rates were adjusted and the transmissivity was measured. The transmissivity measured allowed the determination of the actual dust concentration inside the tube.

4.5 Ignition

For the ignition of the dust/air mixture inside the combustion tube, a spark ignition system was used. Two different setting were used for spark generation, both based on a current transformer and a control circuit. The first assembly created a constant spark with an ignition energy of around 200 mJ. This assembly provided a strong spark on the one hand but proved to be electronically unstable and created an electrical field which disturbed the measuring equipment. Therefore, a spark generator with lower (10 mJ) but stable ignition energy was constructed. The circuit diagram is demonstrated in Figure 34.

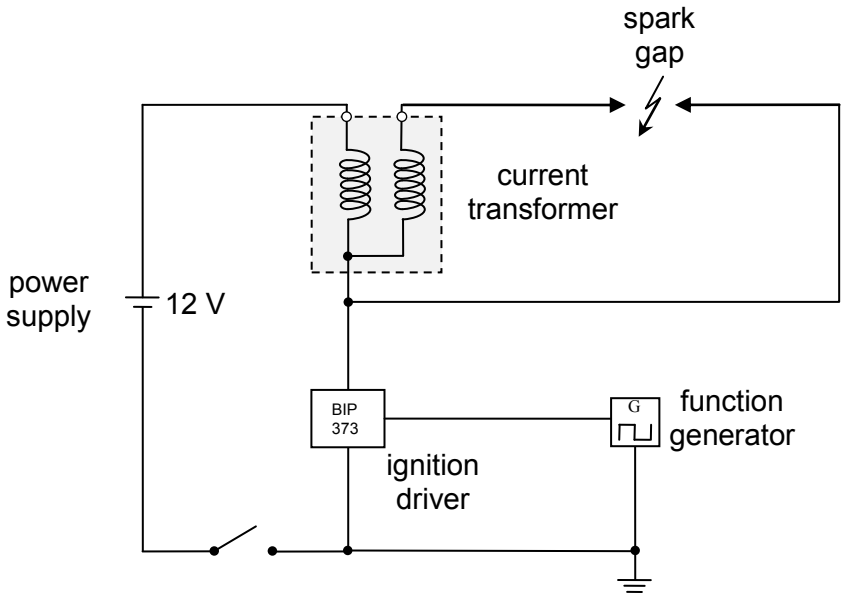

Figure 34: Circuit diagram of the spark generator used for ignition

Two pointed steel-electrodes with a diameter of 2 mm were used as spark igniters. The electrodes were placed such as to form a gap of 6 mm right in the centre of the combustion tube. This electrode assembly is normally also used for dust explosion testing. Experiments with different inert gases were carried out with the stronger ignition source of 200 mJ. For the experiments below ambient pressure the spark generator with lower ignition energy was used.

4.6 Measurement of flame propagation

Considering the characteristics of the flame, optical systems were used for the measurement of flame propagation and flame geometry. Pre-experiments revealed that flames obtained by lycopodium/air mixtures can be observed visually and emit considerable amounts of yellow and red light due to glowing particles.

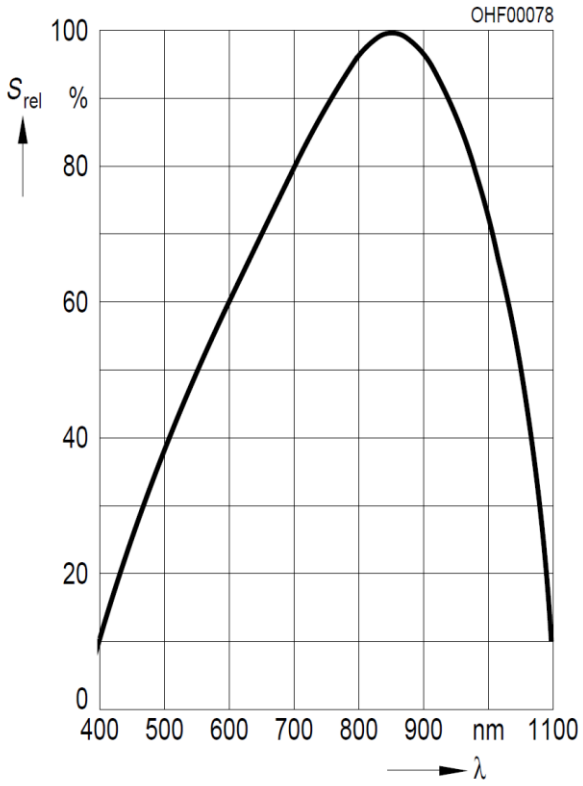

Figure 35: Relative spectral sensitivity of the photodiodes used $S_{rel} = f(\lambda)$ [46]

For the determination of the flame velocity, five BPW 34 silicon photodiodes were placed along the combustion tube. These show a peak in relative spectral sensitivity at around 850 nm, which covers the top end of the spectrum of visible light (780 nm) and also near infrared (Figure 35). The first photodiode was installed 100 mm above the ignition point, all others in steps of 400 mm. Figure 36 provides the directional characteristics of the BPW 34 photodiodes. The photodiodes cover a large angular section, which leads to a pre-detection of the approaching flame front. However, this effect has the disadvantage that the detection signal does not form a sharp peak, which makes the analysis of the signal more difficult and less precise.

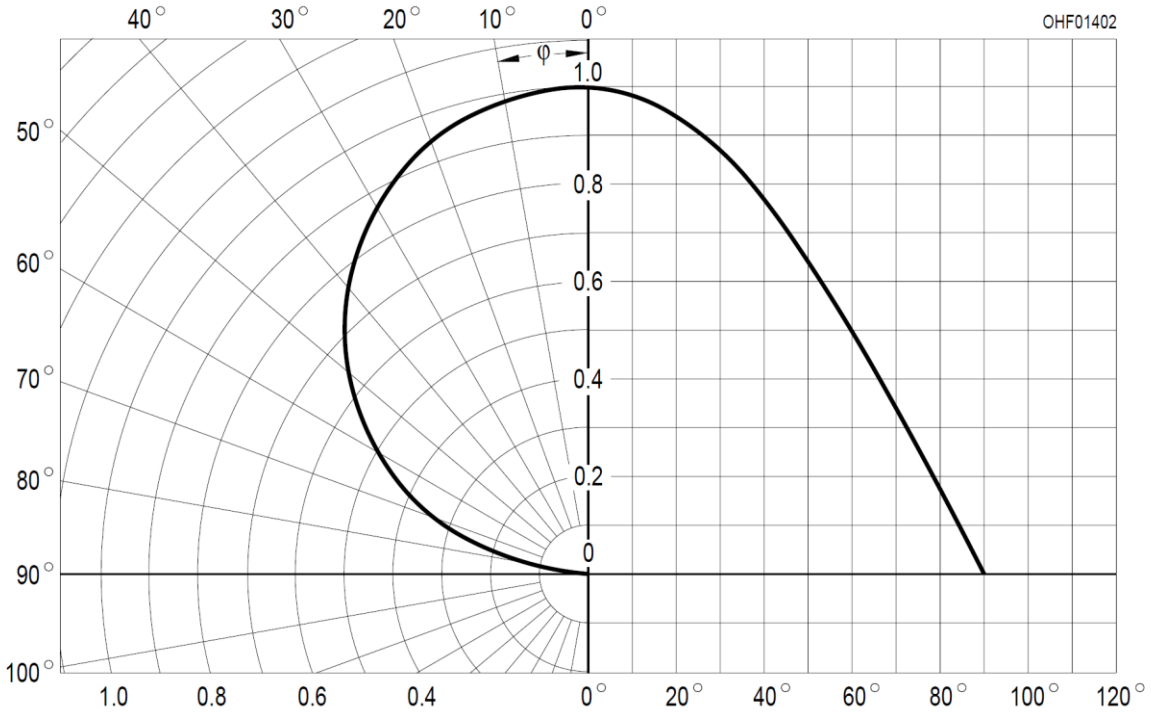

Figure 36: Directional characteristics of the BPW 34 photodiodes $S_{rel} = f(\varphi)$ [46]

For further investigation it proved practical to measure the distances between defined offset points of the signal from the signal ground level. The offset point (P_{Offset}) was defined by the following equation (Eq. 4-2):

$$P_{offset} = Signal + 3\sigma_{signal} \qquad \textbf{(4-2)}$$

The variable σ_{signal} indicates the standard deviation of the signal. The flame velocity was then calculated (Eq. 4-3) out of the time interval between the offset points of the first and the second signal (Δt) and the distance between the photodiodes (Δs).

$$S_F = \frac{\Delta s}{\Delta t} \qquad (4\text{-}3)$$

For calculation of the flame speed only the signal of the first two photodiodes was used. First experiments during construction of the apparatus revealed that the flame undergoes a certain acceleration reaching velocities at the top of the apparatus differing from those in the first section of up to an order of magnitude. Stable values could only be obtained in the first section of the combustion tube. Figure 37 describes the relation between the photodiode signals and actual flame propagation.

The point 0 mm at 0 ms indicates the flame reaching the first photodiode. Around 240 ms later, the second diode at 400 mm is passed by the flame. Compared to the photodiode signals in the picture above, it can be seen that the signal peaks do not represent the location of the flame front.

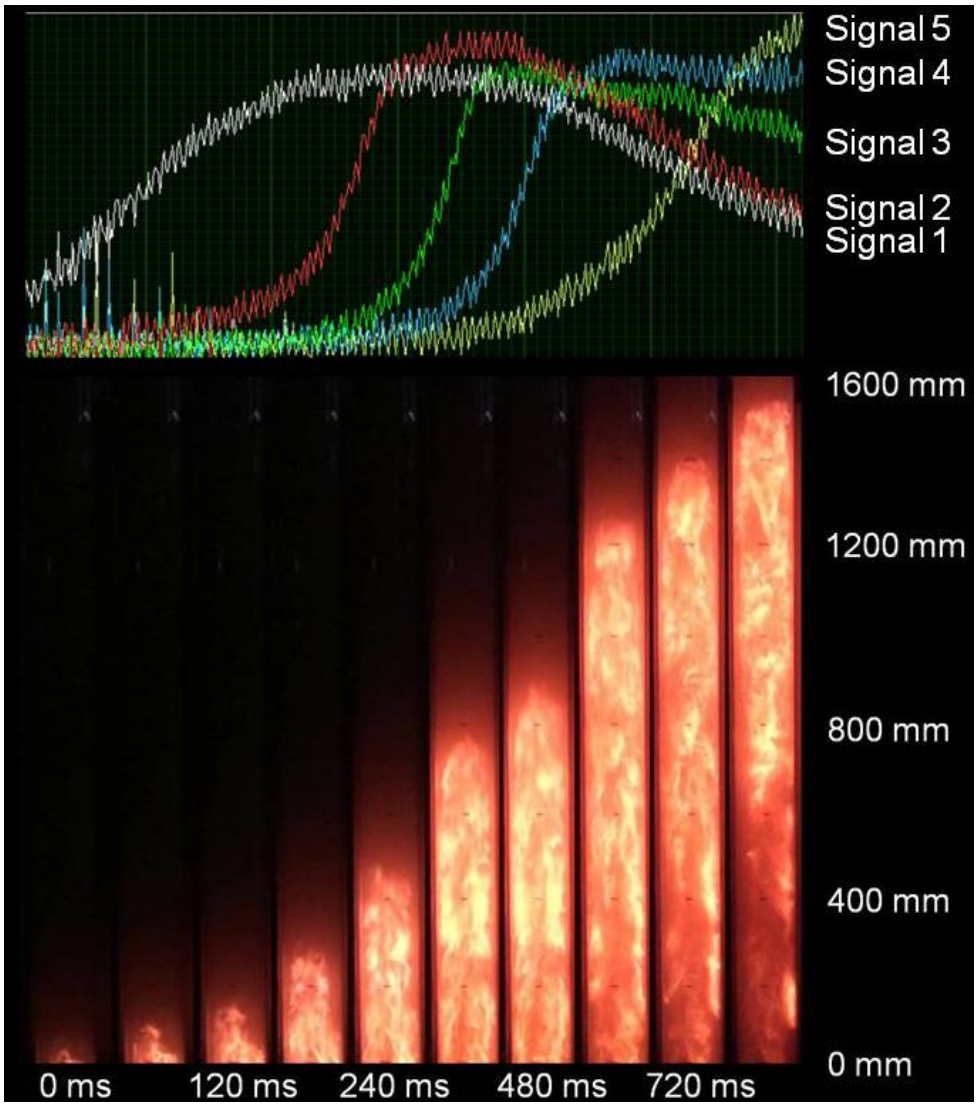

Figure 37: Signal development and flame propagation during an experiment with a dust concentration of 300 g/m³ [47]

5 Flame propagation under non-atmospheric conditions – Results and discussion

The main goal of the present work was to investigate flame propagation under non-atmospheric conditions. Lycopodium spores were used as the test substance. Investigations on phenomenological variations of the combustion process itself as well as the parameter of flame velocity were of special interest. The ignition process was also of certain interest, although in-depth research on its mechanisms was not possible with the chosen experimental setup. Nevertheless, some findings may provide hints for further research on this matter.

5.1 Test substance lycopodium

Lycopodium is commonly used in experiments in dust explosion research. The major advantage of organic spores is the nearly uniform particle size of around 30 µm. Different types of lycopodium spores with slightly different compositions are available. The fuel parameters of the species used for the present study are displayed in Table 5. On the basis of the chemical analysis of a lycopodium sample, the stoichiometric dust concentration at ambient conditions was calculated and found to be 105 g/m³ taking into account the ash and moisture content of the sample. During the evaluation of lycopodium first calculations were carried out on the combustion of lycopodium at different oxygen and fuel concentrations to provide some guiding insights.

Table 5: Fuel parameters of lycopodium

Fuel parameter	
Moisture content	3.3 wt%
Ash content	1.1 wt%
Carbon	64.8 wt%
Hydrogen	9.2 wt%
Nitrogen	1.5 wt%
Sulfur	0,1 wt%
Oxygen (rest)	20.0 wt%
Higher heating value	30000 J/g

With respect to dust explosions, three regimes of combustion are of special interest: stoichiometric combustion, fuel-limited combustion and oxygen-limited combustion. They basically determine the explosive range. Lean combustion in terms of fuel deficiency is characterised by the lower explosion limit (LEL) of the fuel. For lycopodium, different values of the LEL can be found. Calculations based on Schönewald's [17] approach to calculate the LEL, which are mostly based on the calorific value and empirical parameters, revealed values of around 30 g/m³. The GSBL database of the German Umweltbundesamt [48] considers a concentration of 15 g/m³ as "well confirmed" for the LEL of lycopodium. The total combustion of 15 g lycopodium requires ~ 1.3 mol of oxygen, which is equivalent to the oxygen content of 1 m³ air at a pressure of around 150 mbar. For explosion processes at reduced pressure this value was expected to be the limit of combustion due to the lack of oxygen.

Corresponding to that value at ambient conditions is the limiting oxygen concentration, which indicates the limit of flame propagation in terms of oxygen-controlled combustion. The value published for the limiting oxygen concentration of lycopodium lies at 7.5 %Vol. The LOC, is of course, dependent on the dust concentration and the inert gas. Bartknecht [10] found the lowest values for the limiting oxygen concentration, with nitrogen as inert gas, at around 60-70 g/m³ at three different temperatures (20 °C, 100 °C, 200 °C). The amount of oxygen available at that concentration would be sufficient for the total combustion of a dust concentration of around 40 g/m³. Thisleads to the assumption that only around 60 % of the fuel gets oxidised.

Han et al. investigated the weight loss of lycopodium particles at different heating rates and discovered the values shown in Figure 38. At a temperature of around 450 °C, the weight loss of the particles is 60 %. The ignition temperature of lycopodium can be found between 390°C and 440 °C.

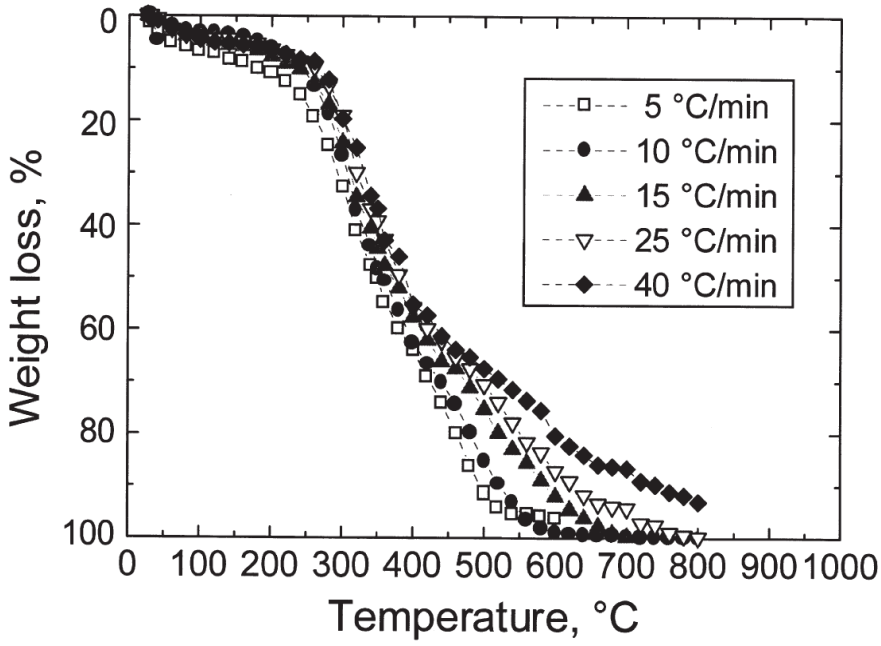

Figure 38: Weight loss of lycopodium particles at different heating rates [37]

As mentioned above, the stoichiometric concentration as calculated lies around 105 g/m³. At a 60 % burn-off rate, the maximum flame speed at ambient conditions is expected at around 170 - 180 g/m³, which is in accordance with Han's results for the laminar flame speed. Investigations in the 20 l Siwek chamber by Skjold [49] showed maximum rates of pressure rise at around 500 g/m³, which indicates an even lower burn-off rate.

5.2 Considerations on the ignition of dust/air mixtures

As described in the previous chapters, the ignition volume or initial flame kernel is strongly linked to basic parameters such as laminar flame speed or minimum ignition energy. For Ignition and flame propagation a critical energy density is necessary, which strongly depends on the heating value of the fuel. Values for ignition volumes are quite rare but support research in the discussion of the fundamentals of ignition. Figure 39 illustrates the development of the ignition kernel in a lycopodium/air mixture at a dust concentration of 100 g/m³. The gap between the electrodes measures 6 mm. The spark generator described in the previous chapter was used (IE~ 10 mJ) for ignition.

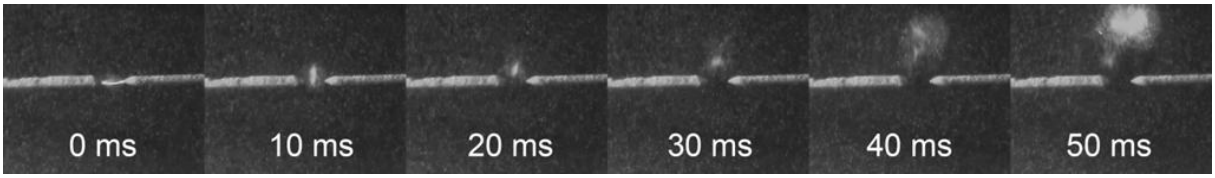

Figure 39: Development of the ignition kernel in a lycopodium/air mixture (100 g/m³)

To suppress luminous effects of the developing flame kernel, the settling particles were illuminated by a slice of green laser light (532 nm) and filmed while using an optical filter (520- 560 nm). As can be seen in the picture sequence, the flame kernel has a diameter of around 4 mm, which is about half the size of the kernel of starch in the initial stage. The flame kernel in the lycopodium/air mixture undergoes the same development as described by Proust [26] for starch/air flames, but reaches only half the size. At the beginning of the ignition process, the flame kernel grows only slowly and hardly changes its size during the first 20 - 30 ms. After that, the flame kernel grows linearly.

Based on the calculations carried out by Proust (2-5) on the relation between the critical flame kernel diameter D_{cr} and the minimum ignition energy, an estimate was done for lycopodium using the flame kernel diameter measured. The thermal conductivity λ of the dust could be neglected due to the circumstance that the volume of the dust is considerably low compared to the total volume. The calculations yielded a minimum ignition energy of 0.5 mJ for lycopodium and 4 mJ for starch. For starch, the result is within the range of the different values that can be found in literature [48] (5- 10 mJ). For lycopodium, it is to low, showing a minimum ignition energy of around 5 mJ and below. Following Skjold's theory that measurement of laminar flame velocities in general will not be successful with present devices because of the strong influence of turbulence also on the micro scale, the minimum

ignition energies calculated by Proust's relation have to show higher values. Calculations were also carried out for lycopodium on the basis of experiments in the Siwek chamber by Spijker et al. [44].

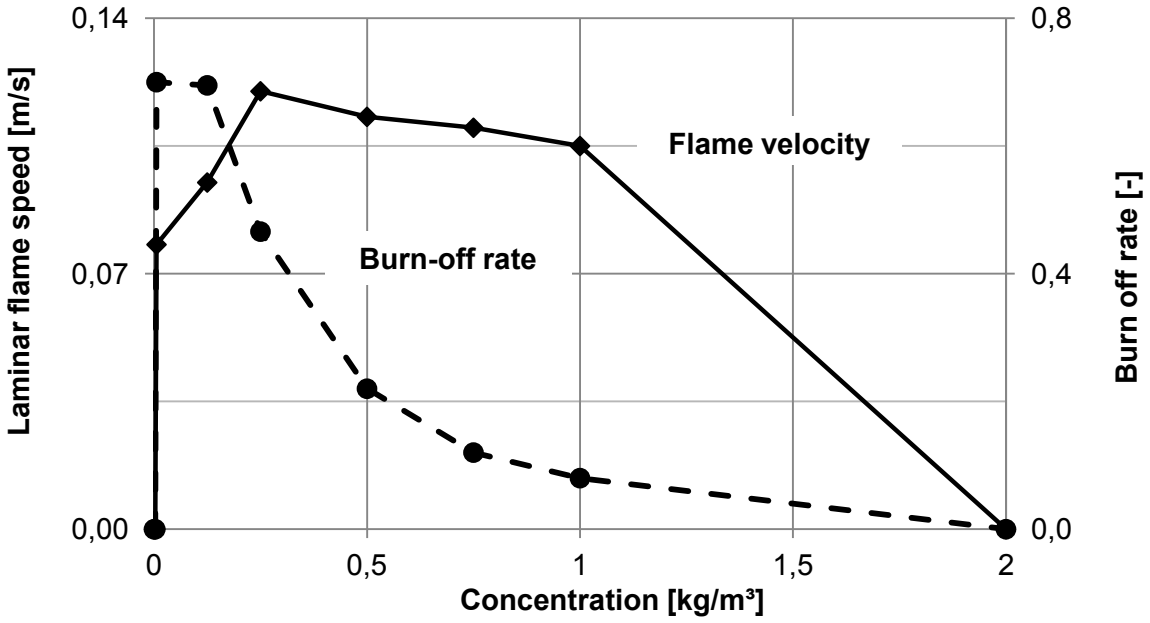

Figure 40: Calculated flame velocity from experiments in the 20 l sphere [44]

The results of the flame velocities calculated can be seen in Figure 40. Values at 0 kg/m³ and 2 kg/m³ have no physical meaning but were set for calculative purposes due to a limited set of experimental data. The flame velocity for lycopodium was also found to be considerably lower than present experimental results, obtained mostly through experiments within combustion tubes.

Table 6: Input parameters for the calculation of the MIE out of the critical flame kernel diameter

	Symbol	Maize starch	Lycopodium
Gas density of air [kg/m³]	ρ_{air}	1.29	
Thermal conductivity of air [W/(m·K)]	λ_{air}	$2.62 \cdot 10^{-2}$	
Adiabatic flame temperature [K]	T_{ad}	$1.30 \cdot 10^{3}$	
Laminar flame velocity [m/s]	S_u	$0.9 \cdot 10^{-2}$	
Flame kernel diameter [m]	D_{cr}	$7 \cdot 10^{-3}$	$3 \cdot 10^{-3}$

Based on these results the calculation of the MIE using Proust's model was carried out to enable further investigation of the relation between the initial flame kernel and the minimum ignition energy. The parameters displayed in Table 6 were used for the calculation. The results of the calculations compared to the values obtained with the higher flame velocities are shown in Table 7.

Table 7: Calculated MIE using different flame speeds

Dust	S_L [m/s]	MIE [mJ]
Starch	0.23	3.6
	0.09	9.3
Lycopodium	0.50	0.5
	0.09	3.0

The results obtained using the lower flame speeds correspond well to the values in literature. The indication that the flame velocities measured in tube reactors are still too high is strongly supported by these results.

5.3 Ignition under reduced pressure conditions

Reduced pressure can be used as an alternative to adding inert gases for the creation of an atmosphere where the occurrence of a dust explosion may not be likely but possible during certain industrial processes. In contrast to changing the composition of the gas phase under atmospheric pressure conditions, a change in the pressure conditions also changes the physical behaviour of the fuel. The test substance lycopodium contains significant amounts of oil. A reduction of pressure can facilitate the production of a combustible vapour fraction, for example. The oils present in lycopodium are mainly long-chained organic acids such as oleic acid or linoleic acid. These oils exhibit very low vapour pressure at ambient conditions (10^{-6} Pa). It was suspected that during the reduction of the pressure some of the oil components of lycopodium would be stripped. Experiments at ambient temperatures where therefore carried out to analyse the head space over lycopodium at different pressures. No oil components were found in the head space. However, at higher temperatures stripping effects are likely and also pyrolysis will be facilitated.

Not only flame propagation but also the igniton process may be affected in the low pressure area. To study the effects on the ignition process, experiments on the structure of the electrical spark which was used as the igniton source were carried out. Subsequently the ignition process itself was studied.

5.3.1 Spark formation

As already described, an electrical arc generator was used to ignite the different dust mixtures. Under atmospheric conditions the spark caused by an electrical discharge is often approximated by a cylindrical volume, especially at low spark energies. Considering the discharge time and the spark energy, energy density can be calculated by estimating the diameter of the approximated cylinder. The discharge under atmospheric conditions is characterised by a very bright and thin spark. The spark diameter increases with the reduction of pressure (Figure 41).

Figure 41: Influence of pressure on spark formation

At around 150 mbar the spark appears light blue with a diameter of 2-3 mm forming a corona discharge with a good visible ion wind. The reduced pressure influences the breakdown voltage of the assembly following the Paschen law. Investigations on the influence of the ion wind on initial turbulence were carried out but proved invisible with the laser tomographic method. Schlieren photography may be lead to different results.

5.3.2 Ignition process

To further investigate the formation of the ignition process under reduced pressure conditions, the initial flame spread was filmed by a high speed camera at different pressures and a dust concentration of around 100 g/m³. At ambient conditions a flame kernel as described above develops around the ignition spark (Figure 42). The flame kernel grows and eventually lifts off from the spark gap due to buoyancy effects of the hot combustion products. After around 80 ms the flame begins to form the parabolic shape that can be observed during advanced flame propagation. The glowing of single particles is only visible on the edges of the flame front. At around 750 mbar the flame kernel exhibits a blue/violet flame colour, single glowing particles become visible and the flame ball increases slightly faster. With further reduction of the pressure, the growth speed increases further. At 550 mbar the flame ball reaches the same diameter around twice as fast compared to ambient conditions. The flame lifts off much more slowly than at ambient conditions, develops around the electrodes exhibits a mostly blue/violet flame with glowing particles. At 300 mbar the flame grows symmetrically around the ingnition gap and shows no buoyancy effects. The upper section of the flame ball is disturbed by sinking particles. Visually, the flame behaves more or less like a combustible gas/air mixture at reduced pressures.

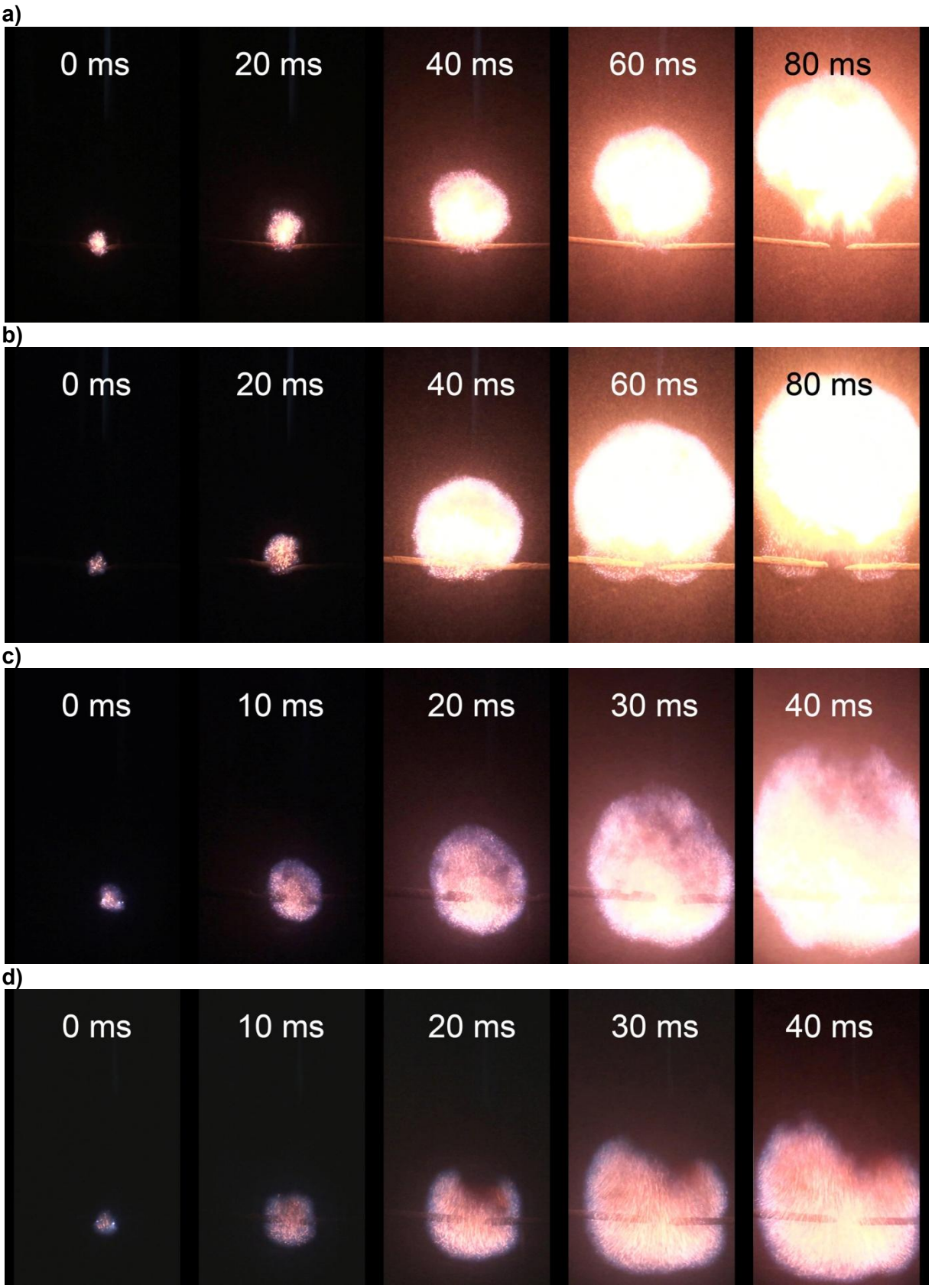

Figure 42: Ignition under reduced pressure conditions at a) 1010 mbar, b) 750 mbar, c) 550 mbar and d) 300 mbar

5.4 Laminar flame propagation in the combustion tube

As described in the previous chapters, a significant problem when trying to measure the laminar flame velocity is the expansion of the combustion products behind the flame front, which accelerate the propagating flame. In order to reduce the influence of the combustion products the assembly described in Figure 28 was used for the experiments. This method had the disadvantage, due to its openings on both ends of the combustion tube, at internal stack effects occurred, which were hard to control. Results obtained from this assembly showed great variance. Nevertheless, it was possible to reach stable conditions for investigations under atmospheric conditions. For the determination of the laminar flame speed Andrews' and Bradley's [36] approach was used. The data necessary to analyse the flame shape was collected via the video analysis system of the apparatus. The flame surface (A_F) and the area cross section (A') were determined and calculated using a Matlab code (Figure 43).

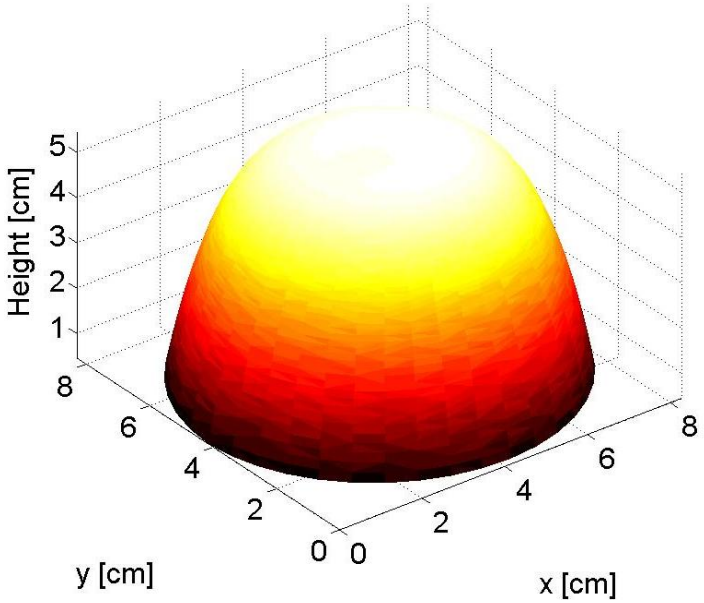

Figure 43: Interpolated flame shape of a 50 g/m³ flame

For a lycopodium concentration of 50 g/m³, the measured flame velocity (S_F) was at 1,29 m/s. Calculations with Andrews' and Bradly's relation resulted in a laminar flame velocity (S_L) of around 0.50 m/s. This value is significantly higher than the value measured by Han et al. for the same concentration (0.35 m/s).

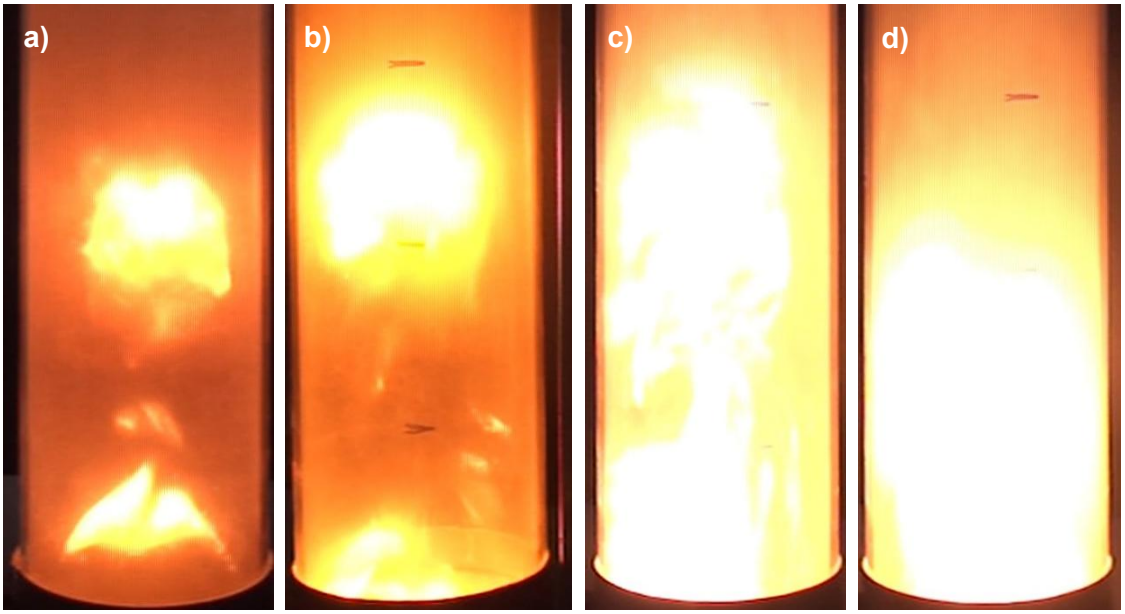

Figure 44: Flame shapes at concentrations of a) 50 g/m², b) 100 g/m³, c) 200 g/m³ and d) 300 g/m³

During the investigations it proved difficult to measure the flame shape, especially at concentrations higher than 150 g/m³, because of considerable big amounts of glowing particles behind the leading flame edge.

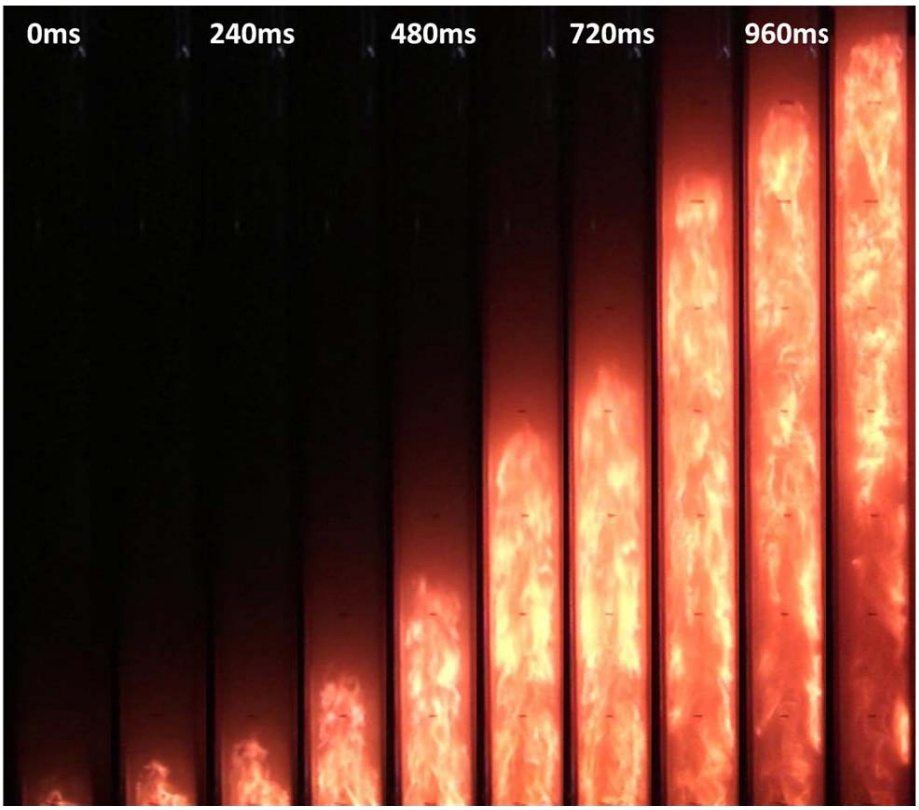

Figure 45: Flame shape and length at a concentration of 300 g/m³

At concentrations of around 50 g/m³, the flame shape was nearly hemispherical. It was significantly stretched at concentrations above 150 g/m³ (Figure 44). Due to the fact that flame shapes at concentrations above 150 g/m³ could not be measured correctly with the chosen method, only flames at lower concentrations were analysed. As described above, an acceleration of the flame was noticed at 400 – 500 mm above the ignition point. This acceleration effect turned out stronger at higher dust concentrations.

As can bee seen in Figure 45, which demonstrates a flame of 300 g/m³, the leading flame front does not form a homogeneous combustion zone right after ignition. After around 500 ms the flame forms a nearly parabolic flame edge. It reaches a total length of around 1000 mm at 960 ms after ignition. For all further investigations on flame propagation only the actual measured flame speed was evaluated because of the problems concerning the determination of the flame shape described above.

5.4.1 Mathematical modelling of the flame propagation in the combustion tube

There is only a limited number of mathematical models available for the simulation of dust explosions [50]. Spijker [44] has developed a model and simulated the combustion process in the experimental setup using the OpenFOAM Software package. Spijker based his model on the assumption of premixed combustible fuel/air mixture described by the variable C. A C value of 1 represents the unburnt mixture, while a value of 0 the completely burnt mixture. The conserving equations for the variable C were solved using the OpenFOAM XiFOAM solver. The XiFOAM solver is used for compressible premixed or partially premixed combustion with turbulence modelling.

Similar to Skjold's method of calculating the laminar flame velocity from results obtained in the 20 l Siwek chamber, Spijker used an approach based on the relation between turbulent and laminar flame velocity described as variable Bsh. Equation 5-1 describes the sub-model used for the description of the combustion process.

$$\frac{\partial(\rho \cdot C \cdot \varepsilon)}{\partial t} + div(\vec{u} \cdot \rho \cdot C \cdot \varepsilon) - div[a_{eff} \cdot grad(C)] = \rho_{unburnt} \cdot S_L \cdot Bsh \cdot |grad(C)| \quad (5\text{-}1)$$

C	Progress variable of combustion
ρ	Density of the gas phase
ρ_{uburnt}	Density of the unburnt mixture
$\vec{u}$	Velocity vector of the gas phase
ε	Volume fraction of the gas phase
a_{eff}	Effective thermal diffusivity
SL	Laminar flame velocity
Bsh	Ratio between laminar and turbulent flame speed

For the description of the dust particles Spijker used an Euler Euler approach to reduce the calculative effort. The equations 5-2 and 5-3 describe the mass transfer between the gas and the particle phase. The actual mass fraction of the fuel taking part in the reaction is represented by the dust concentration c_D and the burn-off rate r_{BO}. The burn-off rate was calculated using Skjold's approach (Figure 40).

$$\frac{\partial(\varepsilon \cdot \rho)}{\partial t} + div\left(\varepsilon \cdot \rho \cdot \vec{u}\right) = \rho_{unbumt} \cdot S_L \cdot Bsh \cdot \left|grad(C)\right| \cdot r_{BO} \cdot c_D \quad (5\text{-}2)$$

$$\frac{\partial(D)}{\partial t} + div\left(D \cdot \vec{u}\right) = -\rho_{unbumt} \cdot S_L \cdot Bsh \cdot \left|grad(C)\right| \cdot r_{BO} \cdot c_D \quad (5\text{-}3)$$

The fraction of oxygen partaking part in the reaction is described by the variable b. The conservation equation for b is given by equation 5-4. The factor f_S represents a stoichiometric factor for the combustion reaction.

$$\frac{\partial(\varepsilon \cdot \rho \cdot b)}{\partial t} + div\left(\varepsilon \cdot \rho \cdot \vec{u} \cdot b\right) - div\left[d_t \cdot grad(b)\right] = - \rho_{unbumt} \cdot S_L \cdot Bsh \cdot \left|grad(C)\right| r_{BO} \cdot c_D \cdot f_S \quad (5\text{-}4)$$

Figure 46 demonstrates the results from the simulation compared to experimental data measured at a lycopodium concentration of 300g/m³.

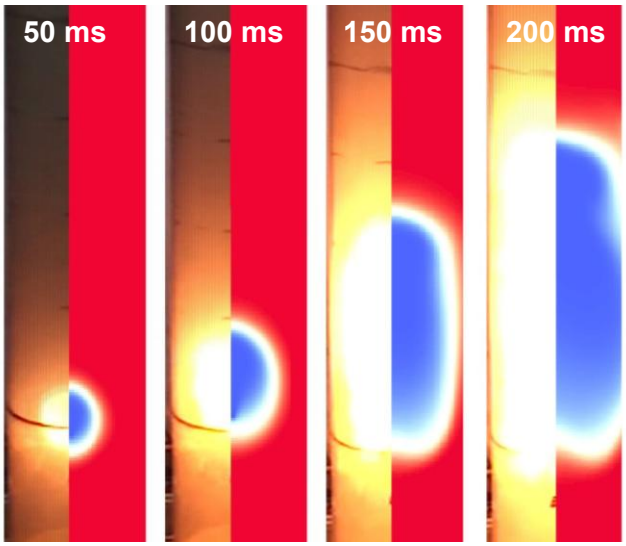

Figure 46: Comparison of experimental flame propagation (left) and results from simulation

The model exhibits good accordance with the experimental data for the observed period of time. Simulations with higher laminar flame velocities as measured only experimentally without turbulence correction, yield results that do not match the experimental data well.

5.5 The Influence of inert gases on flame propagation

Inert gases such as nitrogen or carbon dioxide are commonly used in dust explosion prevention. The key value when using inert gases as a safety measure is the limiting oxygen concentration. The limiting oxygen concentration strongly depends on the inert gas. Therefore the influence of nitrogen and carbon dioxide on flame propagation were investigated and compared with results obtained from experiments in the 20 L sphere.

5.5.1 Experiments on ignition under the presence of inert gases

As described in the previous chapters, inert gases suppress the oxygen concentration on the one hand and act as heat sinks on the other hand. Ignition energy increases exponentially towards the LOC value. Schwenzfeuer et al. [51] have published a model for the calculation of the ignition energy of dust air mixtures based on the minimum ignition energy of a given dust and the oxygen concentration of the mixture (Eq.5-5).

$$IE = MIE \cdot e^{23{,}2-(23{,}2/21)\cdot c_{O_2}} \quad (5\text{-}5)$$

They found that the model yielded good results for minimum ignition energies from 1 mJ up to 1000 mJ and an oxygen concentration between 10 %Vol. and 30 %Vol. Although Schwenzfeuer et al. explicitly stated that the equation should be used only within the given boundary conditions an attempt was made to calculate the limiting oxygen concentration out of known ignition energies. Assuming that there is sufficiently high ignition energy that can be seen as reliable for the determination of whether a dust/air mixture is combustible or not the presented model could be rearranged as to express an oxygen concentration that is theoretically comparable to the LOC (5-6).

$$c_{O_2} = \frac{23.2 - \ln\left(\frac{IE}{MIE}\right)}{\frac{23.2}{21}} \quad (5\text{-}6)$$

In combustible dust testing the ignition energy of 2 kJ can be used in the 20 l Sphere to investigate whether a certain dust/air mixture is explosive or not (VDI 2263 Blatt1). An ignition energy (IE) of 2 kJ was used for the calculations and combined with the given MIE from the BIA Report 12/97 [32]. Table 8 provides an overview on the input data and the results of the calculation for several dusts.

Table 8: Comparison of LOC values from literature sources and calculated limiting oxygen concentrations

	MIE [mJ]	LOC_{lit} [%Vol.]	LOC_{mod} [%Vol.]
Black coal	1000	14.0	14.1
Brown coal	100	12.0	12.0
Wheat flour	30	11.0	10.9
Starch	5	9.0	9.3
Lycopodium	5	7,5	9.3

The calculations show very good results for the coals, wheat flour and starch but only a unsatisfactory value for lycopodium. Lycopodium shows a relatively high minimum ignition energy compared to its limiting oxygen concentration and reactivity in general. To get a

closer view on the ignition behaviour around the limiting oxygen concentration a method based on a modified Hartmann tube was developed. The method was also used to determine and compare the LOC of different dusts with values obtained from the BIA Report 12/97 [19].

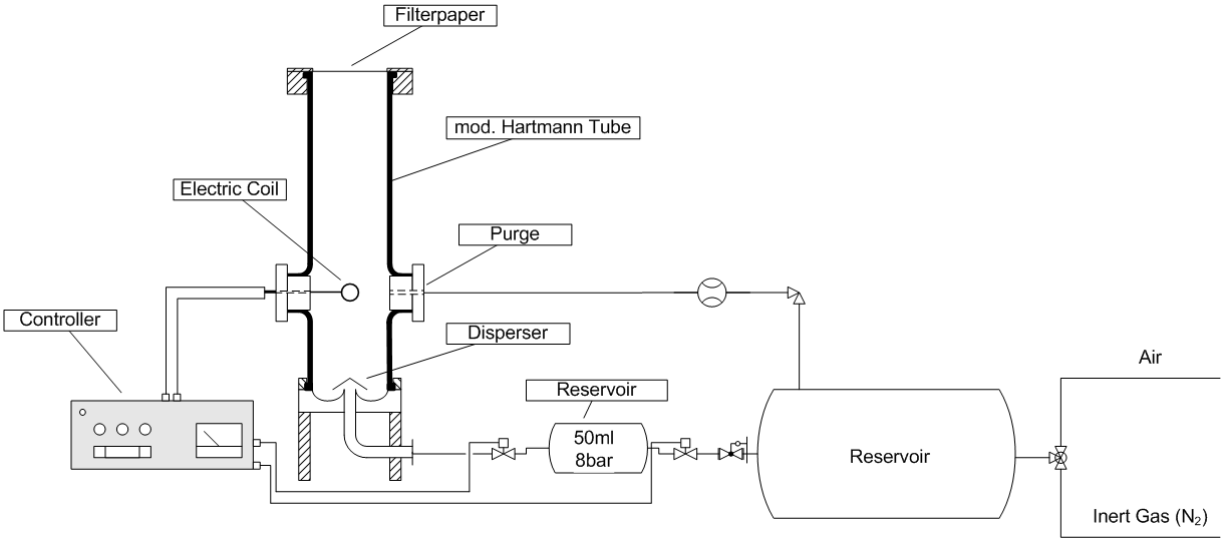

Figure 47: Modified Hartmann Tube for the determination of the LOC

Technically the limiting oxygen concentration and the lower explosion level have in common that they are determined by a limiting factor which does not allow an ignition below a certain value. In case of the lower explosion level the limiting factor is fuel, for the limiting oxygen concentration the limiting factor is oxygen.

In some cases the traditional modified Hartmann Tube with an electrical coil as igniter can be used for the determination of the lower explosion level. In accordance with the testing procedure for the determination of the lower explosion level an existing modified Hartmann Tube was adapted to be able to vary the oxygen concentration within the tube (Figure 47). A comparable experimental setup was also described by Eckhoff.

The modification consisted primarily in the installation of a purge gas system, which allowed variation of atmospheric conditions inside the tube. The Hartmann tube, normally closed with a metal flap, was closed with filter paper containing an opening of 1 cm². A mixing chamber of about 25 liters was installed for sufficient gas supply. The gas was mixed by the partial pressure method and monitored by a gas analyzer. For the Investigations nitrogen was used as inert gas.

The testing procedure was mainly based on the testing procedure conducted in the Hartmann Tube. Autonomous flame propagation after ignition was chosen as the ignition criterion. In accordance with the test procedure for the determination of the minimum Ignition energy, the dust/air mixture was considered not to be ignitable at a certain inert gas

concentration when no ignition in 10 out of 10 experiments could be observed. One minute before the start of the testing procedure and during the testing procedure, the tube was purged with the chosen gas mixture with a purge gas flow of 3 l/min. Measurements showed that the atmosphere inside the tube can be considered as homogeneous after this period of time. According to the EN 14034-4 standard for the determination of the limiting oxygen concentration the oxygen concentration, was lowered in steps of 1 %Vol. until reaching a concentration where no ignition could be observed. This concentration was then marked as the limiting oxygen concentration. All tests were carried out at concentrations from 250 g/m³ up to 750 g/m³.

Table 9: Comparison of LOC values from literature sources and limiting oxygen concentrations measured using the Hartmann Tube

	LOC_{lit} [%Vol.]	LOC_{meas} [%Vol.]
Black coal	14.0	14.0
Brown coal	12.0	12.0
Wheat flour	11.0	10.0
Starch	9.0	9.0
Lycopodium	7,5	8.0

The experimental results showed good accordance with the values obtained from literature. Wheat flour is an exception but an answer may lie in the fact that comparatively large steps of 1%Vol. were used when lowering the oxygen concentration. Therefore, there may be a loss of accuracy.

5.5.2 Flame propagation during nitrogen inerting [47]

As described in the first chapters the limiting oxygen concentration is a certain concentration of oxygen where neither ignition nor autonomous flame propagation can be observed. Bartknecht has discovered that the values for $(dp/dt)_{max}$ exhibit linear decay with increasing nitrogen concentration. Since the maximum rate of pressure rise in a 20 L sphere is strongly linked to the flame velocity, a similar behaviour was expected for experiments regarding flame propagation.

The reaction rate or flame velocity not only depends on the oxygen concentration but also on the concentration of fuel in the mixture. Therefore, concentrations of 100 g/m³, 200 g/m³ and 300 g/m³ were investigated at different oxygen concentrations. The ignition energy of the spark igniter (200 mJ) used provides a comparatively low ignition energy compared to the 10 kJ igniters used in the 20 L apparatus. While using the spark igniter no ignitions were expected at very low oxygen concentrations. Figure 48 shows the results of these experiments with a lycopodium concentration of 100 g/m³. For all oxygen concentrations, a sequence of three tests was carried out. The linear decay of the flame velocity could be observed during the experiments. The flame velocity at ambient conditions was found to be at around 2 m/s. During reduction of the oxygen concentration, the flame velocity dropped to a value of around 1 m/s.

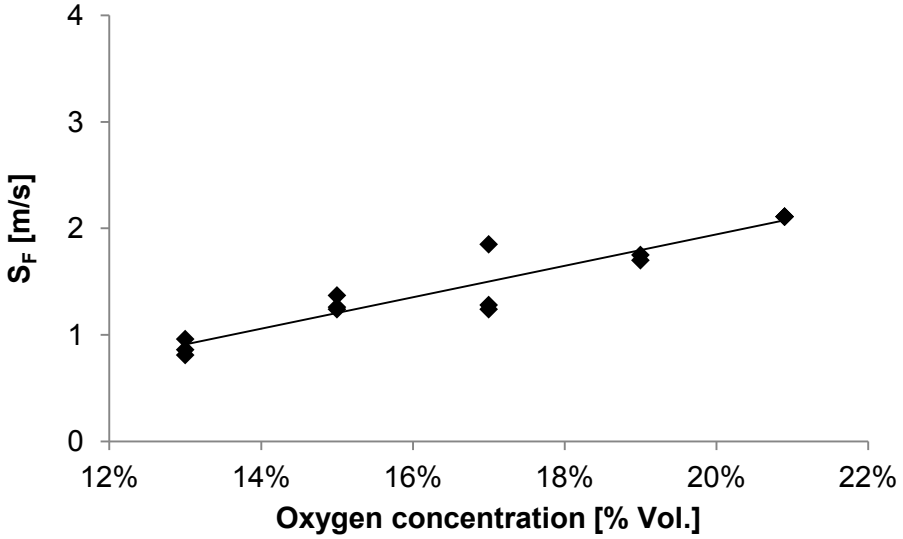

Figure 48: Oxygen concentration vs. flame velocity at 100 g/m³ lycopodium and nitrogen inerting

At oxygen concentrations below 13 %Vol. the ignition of the mixture proved impossible with the used spark igniter. Visually a transition from a closed flame shape to flame propagation with a considerable amount of glowing dust agglomerates could be observed.

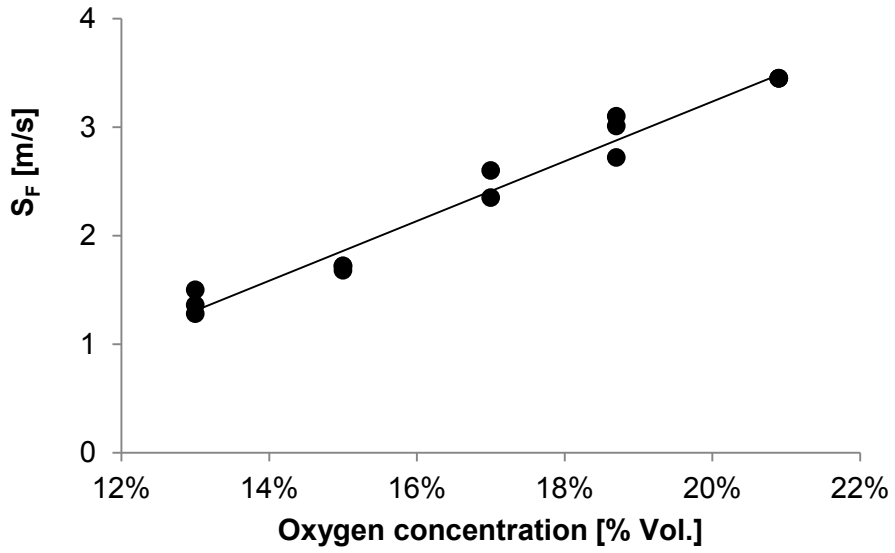

Figure 49: Oxygen concentration vs. flame velocity at 200 g/m³ lycopodium and nitrogen inerting

Flame propagation at 200 g/m³ (see Figure 49) exhibited similar behaviour as described for 100 g/m³ but with increased flame velocities. All values measured showed only little variance. The limit of ignitability was below 13 %Vol. as well.

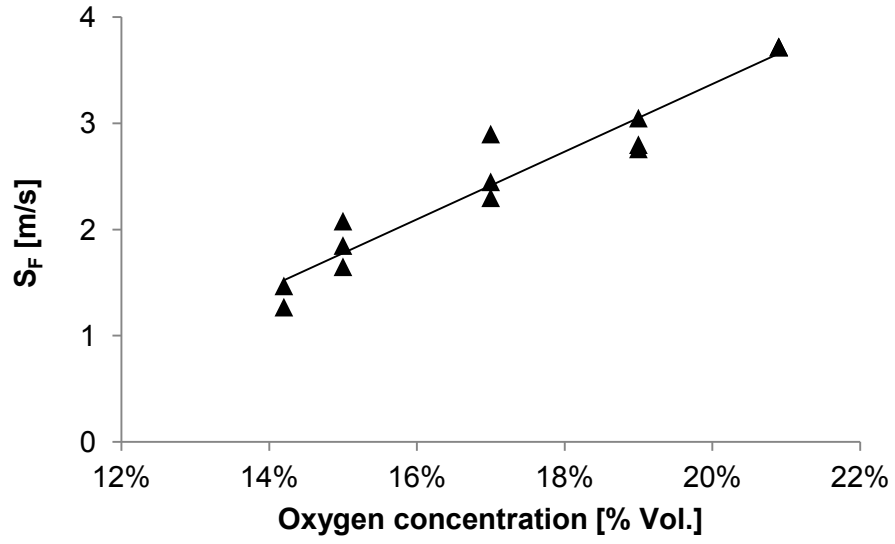

Figure 50: Oxygen concentration vs. flame velocity at 300 g/m³ lycopodium and nitrogen inerting

At 300 g/m³ (Figure 50) slightly higher flame speeds could be measured than at 200 g/m² but the values thus obtained greater variance. Remarkably, the ignition limit shifted from 13 %Vol. to 14 %Vol. This is consistent with Bartknecht's findings that revealed increasing

ignition energies with increased dust concentrations and decreased oxygen contents. The burning of particles or agglomerates was visible at 300 g/m³. The flame formed a more or less closed flame front during all experiments.

In analogy to the determination of the limiting oxygen concentration in the 20 L apparatus, all values measured were plotted in a diagram and extrapolated to S_L= 0 m/s. The strong variation of the values may have been caused by imprecise measurement of the oxygen concentration (Figure 51). Nevertheless, the average value for the extrapolated limiting oxygen concentrations was found to be around 8 %Vol., which is consistent with the value of 7,5 %Vol. published in BIA Report 12/97.

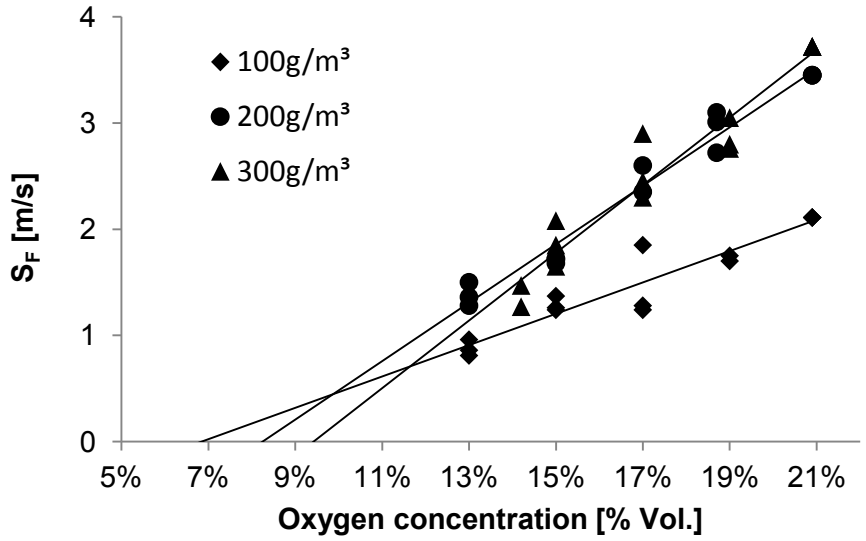

Figure 51: Determination of the limiting oxygen concentration for nitrogen inerting by extrapolation to S_F= 0 m/s

It had been expected that the extrapolated trend lines would intersect at S_F= 0 m/s. This could not be observed. However, the effect of decreasing flame speed by lowering the oxygen concentration became more significant the higher the dust concentration got.

5.5.3 Flame propagation during carbon dioxide inerting [47]

Because of the physical properties of carbon dioxide and Bartknecht's findings, a stronger influence on the flame velocity than by nitrogen inerting was expected during carbon dioxide inerting.

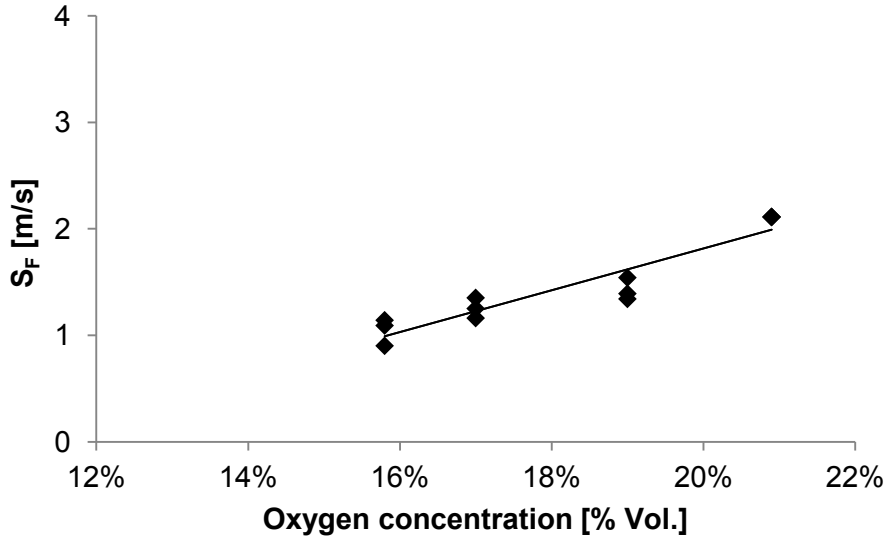

Figure 52: Oxygen concentration vs. flame velocity at 100 g/m³ lycopodium and carbon dioxide inerting

At the first concentration that was investigated (100 g/m³) the drop of the flame velocity caused by the present carbon dioxide was comparable to the effect nitrogen had on the flame propagation. Interestingly, no ignition could be achieved below an oxygen concentration of 16 %Vol. Compared to nitrogen inerting this is an increase of 3% Vol. Furthermore, a continuous electrical spark could not create sufficient energy density to ignite the mixture. During some ignition trials the development of a small flame kernel could be observed, but self sustaining combustion could not be initiated. Figure 52 shows the development of flame velocity when inerting with carbon dioxide. The values at 19 %Vol. of oxygen turned out lower than had been predicted by linear regression. This may be an effect of imprecise measurement of the oxygen concentration. Comparable to nitrogen inerting the flame velocity drop exhibited a steeper decline at a dust concentration of 200 g/m² as it can be seen in Figure 53. The limit of ignitability was again found at 16 %Vol.

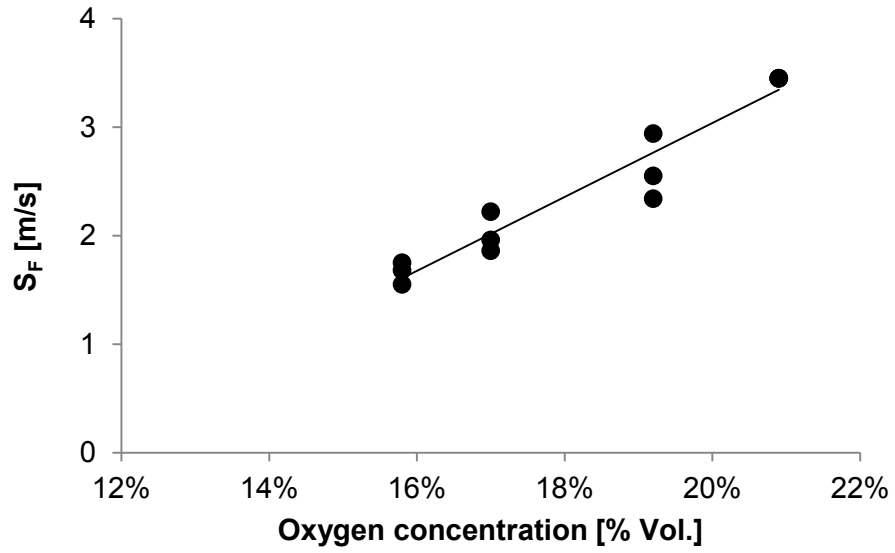

Figure 53: Oxygen concentration vs. flame velocity at 200 g/m³ lycopodium and carbon dioxide inerting

Less homogeneous are the results obtained at a dust concentration of 300 g/m³. This effect can be explained by the generally higher flame velocity and the growing influence of turbulent combustion. Interestingly the limit of ignitability could be found at 15 %Vol., which is 1 %Vol. lower than for the other two concentrations.

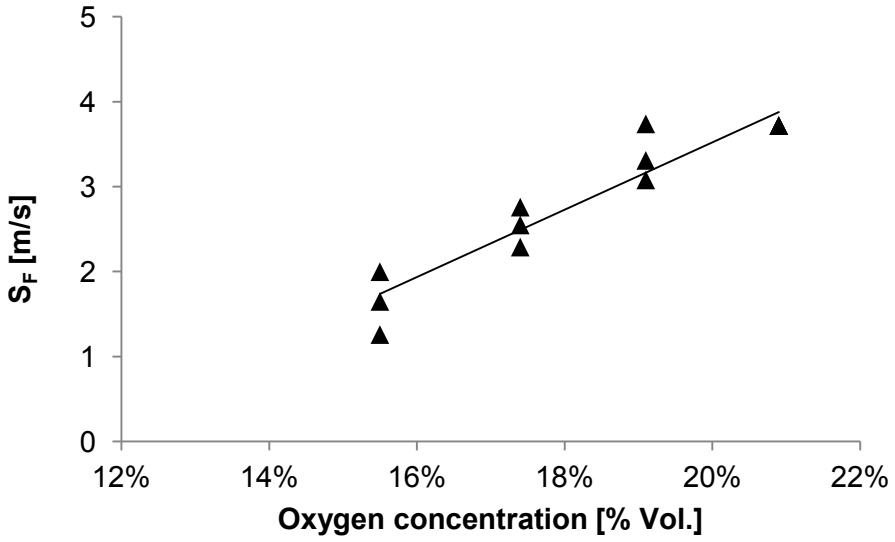

Figure 54: Oxygen concentration vs. flame velocity at 300 g/m³ lycopodium and carbon dioxide inerting

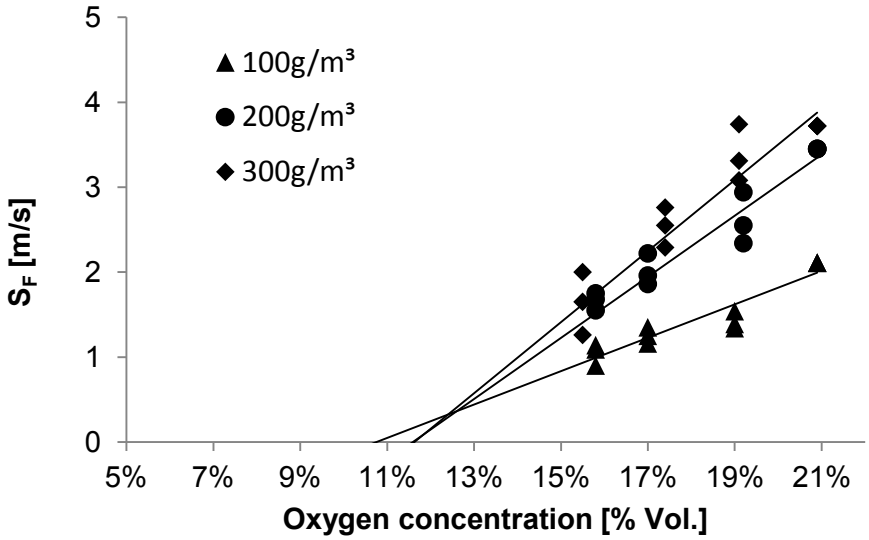

Figure 55: Determination of the limiting oxygen concentration for carbon dioxide inerting by extrapolation to S_F= 0 m/s

As expected for nitrogen inerting the linear regressions of the measured flame velocities exhibit a point of intersection at 11.0 %Vol. and S_F= 0 m/s, which indicates the limiting oxygen concentration during carbon dioxide inerting. For lycopodium, no literature values could be found for the limiting oxygen concentration with carbon dioxide as inert gas. Using Siwek's relation (2-7) the LOC at the presence of carbon dioxide was calculated with 10.2 %Vol.. Taking into account the value of 8 %Vol. measured during nitrogen inerting, Siweks calculation shows a very good agreement.

5.6 Flame propagation under reduced pressure conditions

Due to the findings of the investigation of the ignition process, it was supposed that flame propagation is strongly influenced by pressure conditions. To ensure comparable results, the calibration of the dust feeding system was checked at several pressure levels. With the chosen detection system, no significant variance to the values obtained during experiments at ambient conditions was noticed. The dust was distributing homogenously over the entire cross section of the combustion tube during sinking.

5.6.1 Flame shape

As described in the introductory chapters, combustion idealistically takes place in a thin layer that separates the fuel/air mixture and the products of combustion. The fuel consumption is thus related to the surface area of the combustion zone.

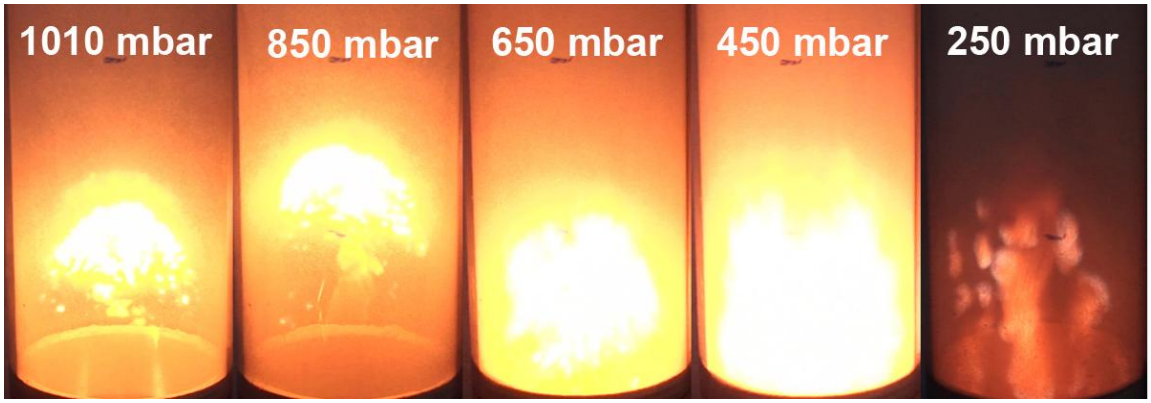

Figure 56: Flame shape at different pressure levels (100 g/m³)

At ambient conditions the flame forms a parabolic shape due to wall effects. During the experiments under reduced pressure conditions, a change in the appearance of the flame of the flame was noticed. The closed flame shape that is formed at ambient pressure becomes distorted with the reduction of pressure (Figure 56). At the given concentration, flames at 450 mbar and 250 mbar show nearly the same flame speed of around 7 m/s but appear visually as completely different. At 250 mbar the flame does not form a uniform flame surface anymore and is dominated by single spot flames. In addition, the light intensity of the flames in the low pressure area is much lower than at ambient pressure, which may be caused by lower combustion temperatures. A determination of the laminar flame velocity with Andrews

and Bradley's approach was not applicable to these flames because of their inhomogeneous flame surface.

5.6.2 Flame speed

Investigations on flame speed were conducted in the apparatus described in Figure 29. For igniting the dust/air mixture the spark generator described (IE ~10 mJ) was used. For the experiments the apparatus was evacuated down to the designated pressure level and ignited after around 30 s of dust feeding to assure homogeneous dust dispersion. Experiments were carried out at dust concentrations of 100 g/m³, 200 g/m³ and 300 g/m³. Figure 57 shows the results of the first set of experiments carried out at 100 g/m³.

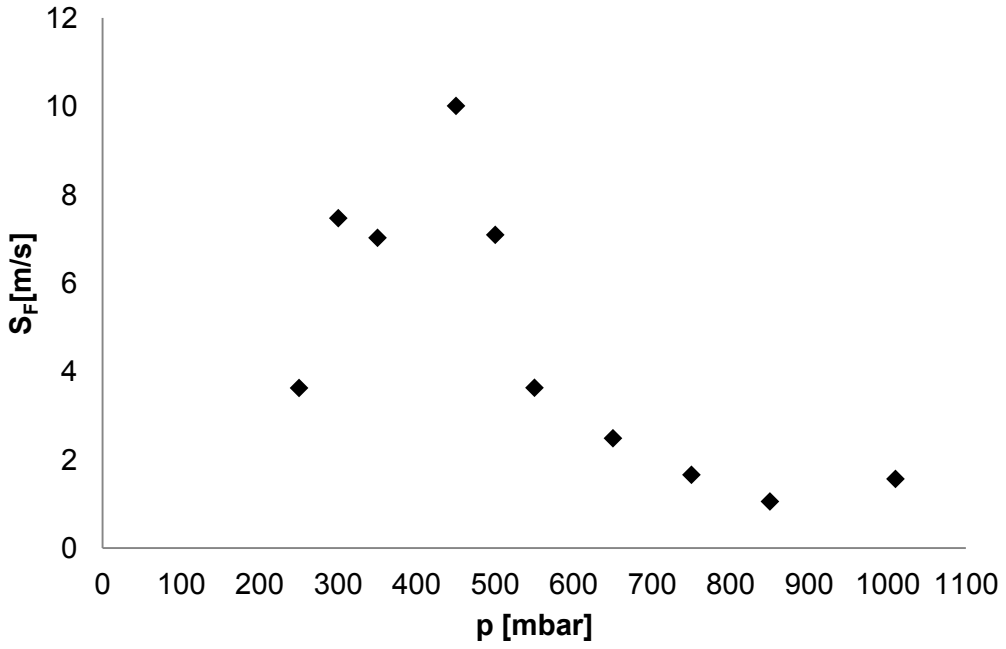

Figure 57: Pressure vs. flame velocity at 100 g/m³ lycopodium [43]

A relatively stable flame speed was found between 1010 mbar and 750 mbar. Below 750 mbar the flame speed increases significantly reaching a maximum at 450 mbar. Further reduction of the pressure slows down flame propagation. With the spark generator used, igniton below a pressure of 250 mbar was impossible. As described above, the formation of a parabolic flame shape was not observed at very low pressures. The considerably high flame speed and the not very bright flame also led to a stronger variation of the values measured at reduces pressures.

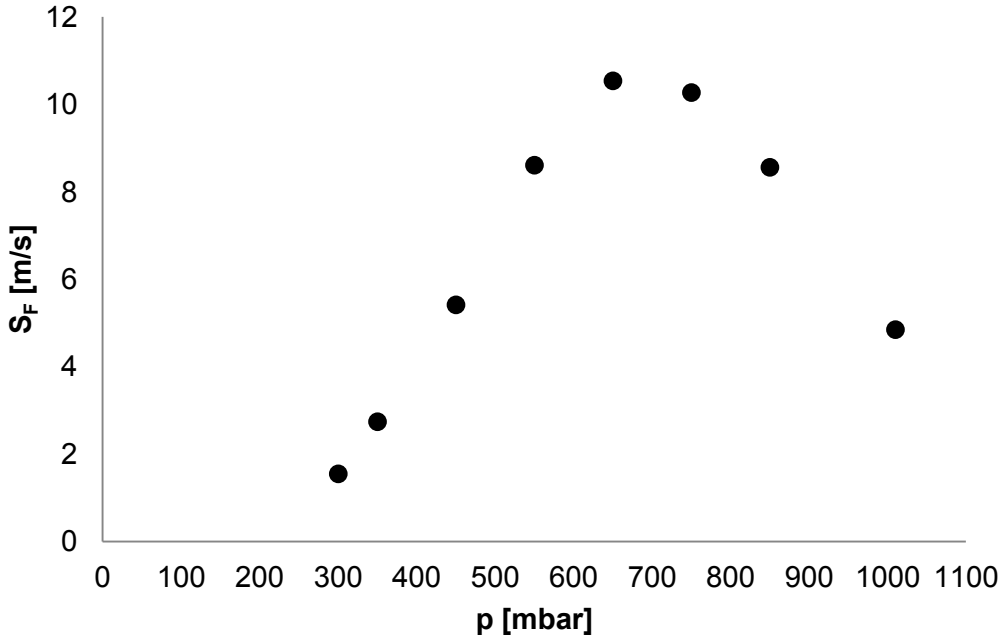

Figure 58: Pressure vs. flame velocity at 200 g/m³ lycopodium [43]

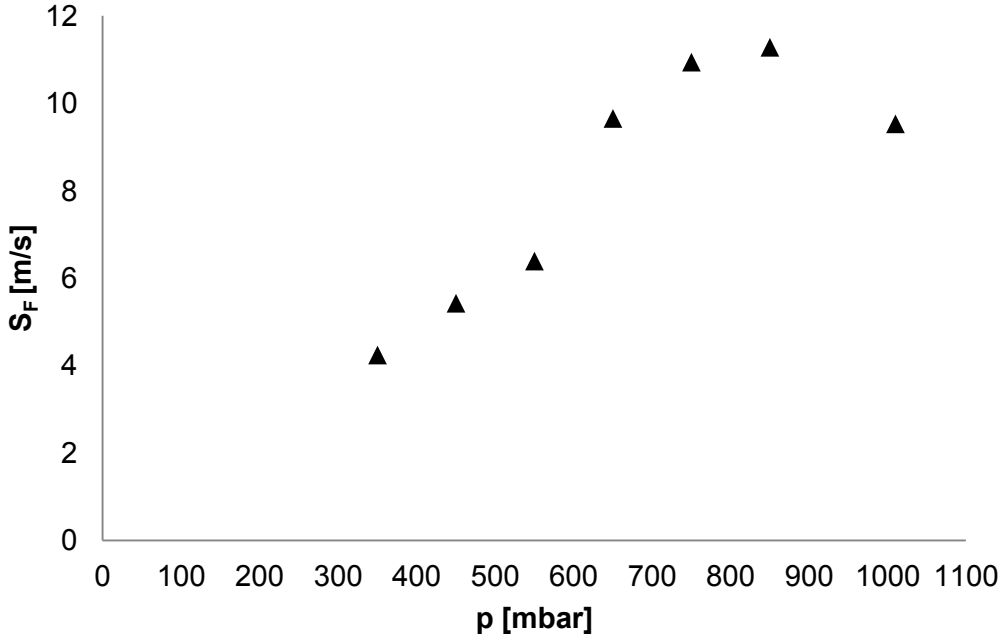

Figure 59: Pressure vs. flame velocity at 300 g/m³ lycopodium [43]

Figure 58 demonstrates of the results the flame speeds measured at a concentration of 200 g/m³ lycopodium in air during the reduction of pressure. Corresponding to the previous set of experiments, the flame speed rises during the reduction of pressure. A section of constant flame speed was not found. Maximum flame speed was observed at around 650 mbar. Ignition became impossible at a pressure of 300 mbar. As can be seen in Figure 59, the maximum of the flame speed shifted further towards ambient pressure when the dust concentration was raised to 300 g/m³. The limit of ignitability shifted further and was reached at 350 mbar.

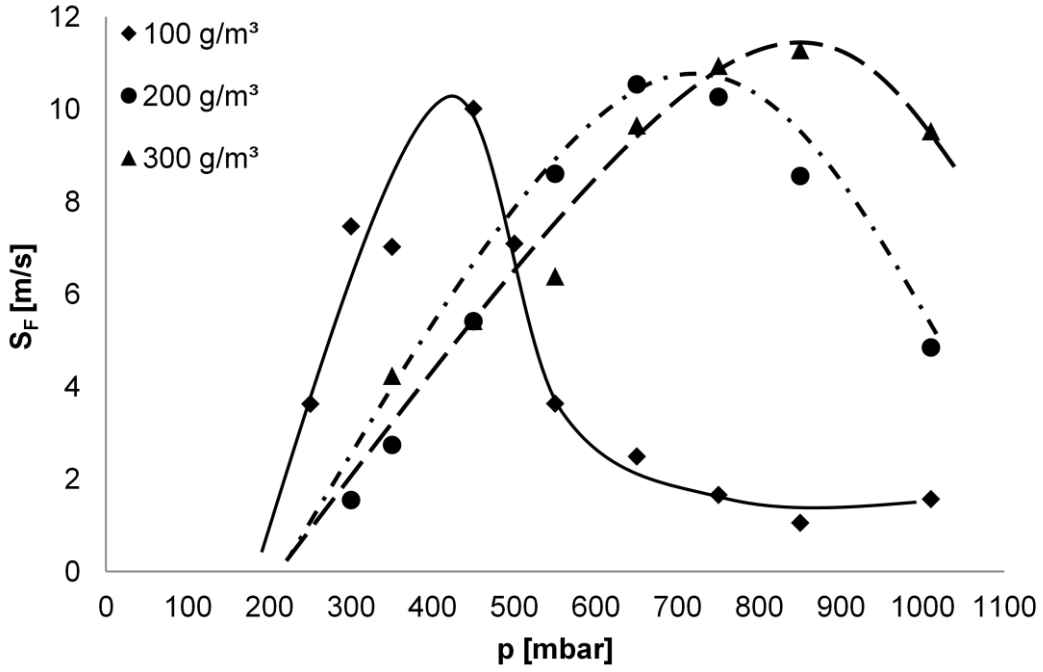

Figure 60: Pressure vs. flame velocity at 100 g/m³, 200 g/m³ and 300 g/m³ lycopodium

A comparison of all three datasets reveals that maximum flame velocities can be achieved at different pressures depending on the fuel concentration (Figure 60). The slope of the increasing as well als the decreasing flank of each curve also varies with the dust concentration. The curve at 100 g/m³ is more narrow than at the other two concentrations. The curves spread with increasing dust concentrations. Interestingly, the falling flanks of all three curves seem to join at a value of around 200 mbar when extrapolated. 1 m³ of air at 200 mbar contains the amount of oxygen that is necessary for the total combustion of 20-25 g of lycopodium. The lower explosion level of lycopodium lies right in this area. Therefore, the result seems consequent.

6 Summary, conclusion and future prospects

In the course of this work, several methods for the determination of the laminar flame velocity as a fundamental parameter of flame propagation have been studied and evaluated. Experimental methods had to be found which allowed to reach the main goal of the study, the determination of the behaviour of lycopodium/air mixtures under conditions deviating from ambient conditions. The following paragraphs contain concluding remarks and prospects for further research on this matter.

6.1 Summary

For this work different apparatuses for the determination of the laminar flame velocity under non-atmospheric conditions have been developed and tested. It had already been known that the investigation of flame propagation and flame shape requires a system that allows proper dispersion of the test substance within the apparatus and creating very low turbulence levels. The method chosen to reach low turbulence conditions in the entire combustion area was that of a conveyor screw assembly combined with the natural gravitational settling of the dust. During the course of the study test substances such as maize starch should were considered. However, due to their natural tendency of agglomeration, only lycopodium could be used for the experiments. Lycopodium has the huge advantage of a nearly uniform particle size. Its disadvantage is its heterogeneous composition containing solid structures as well as oily components. Nevertheless, lycopodium is commonly used in dust explosion research and allowed the comparison of the experimental values with several sources from literature.

The first attempts to determine flame velocity were dominated by fulfilling the requirements of safe experimental conditions. First experiments were therefore carried out as field experiments outside the laboratory using a completely open top end of the chosen combustion tube. The method was not deployable to laboratory surroundings, which is why in-built safety devices had to be used. However, these later on also seemed to influence the results due to the creation of a certain flow resistance. Experiments with an open bottom end of the experimental device could not provide reproducible results over a large range of dust concentrations. The calculation of the laminar flame velocity out of the experimental results was possible for low concentrations but not successful for concentrations above 150- 200 g/m³. It was therefore decided to use the uncorrected actual flame speed as the parameter for further investigations on flame behaviour. The spark generators especially constructed for the purpose of ignition proofed to be reliable and fulfilled the experimental needs.

In addition to the video analysis system, an optical measurement system based on photodiodes was used for the determination of the flame speed. The diodes had the disadvantage of a big angular field of view that did not allow an exact determination of the approaching flame front and therefore proved a source of error. Statistical methods were used to create reliable results but the method still shows deviations of up to +/- 1 m/s, especially at higher flame speeds. The results are also influenced by the light intensity of the flame. All things considered, flame speeds of all three experimental assemblies as measured were higher than comparable results found in literature. Nevertheless, most of the experimental apparatuses suggested do not allow to measure flame speed under the specific conditions chosen for this work.

From the phenomenological perspective the description of the ignition process under the influence of inert gases and under reduced pressure conditions were also of interest. The formation of an initial flame kernel is strongly linked to basic parameters such as minimum ignition energy or the flame velocity. The application of different mathematical models combined with experimental data related to the ignition and combustion process revealed that the methods used for the determination of the flame velocity in tube reactors produce values that are too high. Methods for calculation of the laminar flame speed out of results obtained in the 20 l Siwek chamber are available but still not investigated in depth and therefore cannot replace present safety-relevant parameters.

Another problem with safety relevant parameters is that only few of these parameters are available for non atmospheric conditions. The limiting oxygen concentration was determined for several dusts but flame propagation under low pressure conditions is still poorly investigated. Experiments with different inert gases showed that the flame velocity behaves

similarly to the maximum rate of pressure rise measured in the 20 l Siwek chamber when inert gases are present. The flame velocity drops linearly towards a certain oxygen concentration where the flame speed reaches the theoretical value of 0 m/s. This effect could be observed very well with the experimental device used. The values also showed good accordance with literature data.

The experiments below atmospheric conditions revealed effects that had not been predictable in the first place. Flame speeds generally increased during pressure reduction up to a certain peak value and decreased after passing that maximum speed. Flame speeds measured at low pressure conditions reached an order of magnitude higher than at ambient conditions for the investigated dust concentrations of 100 g/m³, 200 g/m³ and 300 g/m³. The velocity maximum shifted towards atmospheric pressure with increasing dust concentrations. Results of comparative calculations based on safety relevant parameters determined at ambient conditions agreed with these findings.

Of special interest was the investigation of the ignition behaviour under reduced pressure conditions. For example, the effect of buoyancy of hot gases at the initial stages of ignition normally observed at ambient conditions was not predominant at low pressures. The flame kernel grew symmetrically around the spark gap and the appearance of the flame was also more comparable to a gas flame. Temperature readings were not installed. Determination of the reaction kinetics is based on the present data set not possible therefore.

6.2 Conclusion and future prospects

Safety-relevant parameters are commonly used for the evaluation and characterisation of hazardous substances. They still form the basis of hazard analysis within industrial processes. It is already known that these safety-relevant parameters are strongly influenced by the experimental method. Standard apparatuses feature certain limitations in the variation of experimental conditions. Therefore, there is a need for new methods of hazard evaluation originating from a knowledge-based approach.

Flame velocity is not a very common parameter for the evaluation of combustible dust/air mixtures, but the experimental settings also chosen in this work allow the variation of gas compositions as well as the reduction of pressure. In contrast to present testing equipment, the equipment used for this study allowed a closer look at the combustion process itself. It was possible to investigate the influencing parameters on and the conditions at the ignition process in a more detailed way than possible with the 20 l Siwek chamber or the MIKE 3

apparatus. New results have been found on flame propagation and ignition at low pressure conditions. These results may not be applicable directly to a practical problem set but enable further research on the mechanisms and influencing parameters of the combustion process. From the knowledge thus gained, theories of combustion processes under atmospheric conditions can be improved or established.

The experimentally determined laminar flame velocity will probably not replace present standard testing methods but contributes to the understanding of explosion processes. The investigation of the reaction kinetics of the combustion reaction or a deeper investigation of the ignition process should benefit especially from being studied with slow and steady flames. The flame velocity is therefore a parameter worth being investigated further.

During the course of work, several ideas for further research on this matter as well as measures for improvement came up. Besides lycopodium, the investigation of other dusts as well as the analysis of reaction mechanisms differing from the combustion of lycopodium should be carried out. The method of dust dispersion described in this study is only applicable to a very limited number of dusts. Therefore, a new design of the dispersion system would be helpful.

The measurement of combustion temperatures was not possible with the chosen experimental setup, but would contribute to a better description of the combustion process [28] [9] [10] and kinetics. The video analysis system used during the experiments proved to be ineffective at higher dust concentrations. The determination of the flame surface was only possible at lower concentrations. High speed video takes were only possible at around 100 frames per second. The use of a high-speed camera with a higher frame rate combined with an improved laser tomographic system would improve the reliability of the results. A lot of experimental uncertainty was also created by the optical measurement system for the flame speed. The velocity measuring system as well as the dust concentration measurement should be improved in future works.

An increasingly important factor in future research will be the mathematical modelling of dust explosion processes. New methods for experimental characterisation combined with mathematical modelling will enhance safety in industrial processes.

7 Resources

[1] NIOSH, Milestones in Mining Safety and Health Technology, NIOSH Technology News (2002), 495.

[2] U.S. Department of Labor, Federal Coal Mine Health and Safety Act of 1969, Public Law (1969).

[3] VDI 2263, Staubbrände und Staubexplosionen, Gefahren-Beurteilung-Schutzmaßnahmen (05.92), Beuth-Verlag, Berlin, 1992.

[4] U.S. Chemical Safety and Hazard Investigation Board, Sugar Dust Explosion and Fire, 2009.

[5] Steinbach, J., Chemische Sicherheitstechnik, WILEY-VCH, Weinheim, 1995.

[6] U.S. Chemical Safety and Hazard Investigation Board, Aluminum Dust Explosion, 2005.

[7] Siwek, R., Determination of technical safety indices and factors influencing hazard evaluation of dusts, Journal of Loss Prevention in the Process Industries 9 (1996), 1, 21–31.

[8] Cesana, Ch., Siwek, R., Handbuch Mike3, http://www.kuhner.com/tl_files/kuhner/product/safety/PDF/B021_070.pdf, abgerufen am 10. Mai 2013.

[9] Holbrow, P., Wall, M., Sanderson, E., Bennett, D., Rattigan, W., Bettis, D., Gregory, D., Fire and explosion properties of nanopowders, Buxton, 2010.

[10] Bartknecht, W., Zwahlen, G., Explosionsschutz, Springer, Berlin [etc.], op. 1993.

[11] Denkevits, A., Dust Explosion Experiments - Measurements of Explosion Indices of Graphite Dust in Hydrogen-Containing Atmospheres, 2005.

[12] ÖNORM 14034-1, 01.06.2005, Bestimmung der Explosionskenngrößen von Staub/Luft- Gemischen Teil1: Bestimmung des maximalen Explosionsdruckes pmax von Staub/Luft-Gemischen.

[13] Cesana, Ch., Siwek, R., Handbuch 20-l-Apparatur, http://www.kuhner.com/tl_files/kuhner/product/safety/PDF/B000_070.pdf, abgerufen am 30. März 2013.

[14] NFPA 68, 2013, Standard on Explosion Protection by Deflagration Venting.

[15] Steen, H., Handbuch des Explosionsschutzes, WILEY-VCH, Weinheim, 2000.

[16] Cashdollar, K. L., Coal dust explosibility, Journal of Loss Prevention in the Process Industries 9 (1996), 1, 65–76.

[17] Schönewald, I., Vereinfachte Methode zur Berechnung der unteren Zündgrenze von Staub/Luft-Gemischen, Staub - Reinhaltung der Luft 31 (1971), 9, 376–378.

[18] ÖNORM 14034-4, 01.06.2005, Bestimmung der Explosionskenngrößen von Staub/Luft- Gemischen Teil 4: Bestimmung der Sauerstoffgrenzkonzentration SGK von Staub/Luft-Gemischen.

[19] Krause, U., Weinert, D., Wöhrn, P., Rechnerische und graphische Bestimmung der Sauerstoffgrenzkonzentration explosionsfähiger Staub/Luft-Gemische, Staub - Reinhaltung der Luft 52 (1992), 361–368.

[20] Farrell, T.M., Vingerhoets, J., Snoeys, J., Going, J.E., Dust Flame Propagation in Industrial Scale Piping - Part 1: Empirical Study in a Conveying Vessel- Pipeline System, Proceedings of the 9th Global Congress on Process Safety (2013).

[21] Brandes, E., Thedens, M., Kenngrößen des Explosionsschutzes bei nichtatmosphärischen Bedingungen, PTB Mitteilungen 113 (2003), 3.

[22] Warnatz, J., Maas, U., Dibble, R. W., Verbrennung, Springer, Berlin Heidelberg New York, 2001.

[23] Lewis, B., von Elbe, G., Combustion, Flames, Explosions of Gases, Academic Press Inc., New York, 1951.

[24] Zehn, G., Leuckel, W., Effects of ignitors and turbulence on dust explosions, Journal of Loss Prevention in the Process Industries 10, 5-6, 317–324.

[25] Jost, W., Explosion and Combustion Processes in Gases, McGraw-Hill, 1946.

[26] Proust, C., A few fundamental aspects about ignition and flame propagation in dust clouds, Journal of Loss Prevention in the Process Industries 19 (2006), 104–120.

[27] Proust, C., Formalisation du savoir et des outils dans le domaine des risques majeurs, 2006.

[28] van der Wel, P. G. J., Ignition and propagation of dust explosions, Dissertation, Delft University, Delft, 1993.

[29] Kalkert, N., Theoretische und Experimentelle Untersuchungen der Explosionskenndaten von Mischungen aus mehreren gas- und staubförmigen Brennstoffkomponenten und Luft, Dissertation, Universität Dortmund, Dortmund, 1980.

[30] Enstad, G., Effect of Shock Wave Emitted from Electric Spark Discharges on the Energy Required for Spark Ignition of Dust Clouds, Bergen, 1981.

[31] Siwek, R., Zuverlässige Bestimmung explosionsschutztechnischer Kenngrößen in der 20l-Laborapparatur, VDI Berichte (1989), 701, 215–262.

[32] Beck, N., Glienke, N., Möhlmann, C., BIA- Report 12/97 Brenn- und Explosionskenngrößen von Stäuben, Sankt Augustin, 1997.

[33] Jost, W., Explosions- und Verbrennungsvorgänge in Gasen, Springer, Berlin, 1939.

[34] Joos, F., Technische Verbrennung, Springer-Verlag Berlin Heidelberg, Berlin Heidelberg, 2006.

[35] Dahoe, A. E., Zevenbergen, J. F., Lemkowitz, S. M., Scarlett, B., Dust explosions in spherical vessels: The role of flame thickness in the validity of the ‘tube-root law’, Journal of Loss Prevention in the Process Industries 9 (1996), 1, 33–44.

[36] Andrews, G.E., Bradley, D., The burning velocity of methane-air-mixtures, Combustion and Flame 18 (1972), 133–153.

[37] Han, O. S., Yashima, M., Matsuda, T., Matsui, H., Miyake, A., Ogawa, T., A study of flame propagation mechanisms in lycopodium dust clouds based on dust particles’ behavior, Journal of Loss Prevention in the Process Industries 14 (2001), 153–160.

[38] Eckhoff, R. K., Dust explosions in the process industries, Butterworth-Heinemann, Oxford [u.a.], 1997.

[39] Palmer, K. N., Tonkin, P. S., Coal dust explosions in a large-scale vertical tube apparatus, Combustion and Flame 1971, 17, 159–170.

[40] Han, O. S., Yashima, M., Matsuda, T., Matsui, H., Miyake, A., Ogawa, T., Behaviour of flames propagating trough lycopodium dust clouds in a vertical duct, Journal of Loss Prevention in the Process Industries 2000 (13), 449–457.

[41] Skjold, T., Selected Aspects of Turbulence and Combustion in 20- Litre Explosion Vessels, Dissertation, University of Bergen, Bergen, 2003.

[42] Wimmer, B., Experimentelle Ermittlung der laminaren Flammengeschwindigkeit brennbarer Staub/Luft Gemische, Master Thesis, Montanuniversität Leoben, Leoben, 2013.

[43] Wieser, G., Untersuchung der Flammenfortpflanzung in Staub/Luft-Gemischen unter reduzierten Druckbedingungen, Master Thesis, Montanuniversität Leoben, Leoben, 2013.

[44] Spijker, C., Kern, H., Held, K., Raupenstrauch, H., Modelltechnische Erfassung von Staubexplosionen, Book of Abstracts zum 9. Minisymposium der Verfahrenstechnik (2013), 211–215.

[45] Scheid, M., Experimentelle Untersuchungen zum Ablauf von Gas- und Staubexplosionen in druckentlasteten Reaktionsgefäßen, Dissertation, Martin-Luther-Universität Halle-Wittenberg, Halle (Saale), 2005.

[46] Siemens, Technical Documentation of Silizium PIN Fotodiodes BPW 34, abgerufen am 01. Oktober 2013.

[47] Kern, H., Held, K., Raupenstrauch, H., Investigations on the influence of the oxygen concentration on the flame propagation in lycopodium/air mixtures.

[48] Umweltbundesamt, GSBL-Gemeinsamer Stoffdatenpool Bund/Länder (Datenbank), http://www.gsbl.de/gsblweb30/main.do, abgerufen am 25. September 2013.

[49] Skjold, T., Arntzen, B.J., Hansen, O.R., Taraladset, O.J., Storvik, I.E., Eckhoff, R.K., Simulating dust explosions with the first version of DESC, Process Safety and Environmental Protection (2005), 83, 151–160.

[50] Di Benedetto, A., Russo, P., Thermo-kinetic modelling of dust explosions, Journal of Loss Prevention in the Process Industries 20 (2007), 303–309.

[51] Schwenzfeuer,K., Glor, M., Gitzi, A., Relation between ignition energy and limiting oxygen concentrations for powders, Proceedings of the 10th International Symposium Loss Prevention and Safety Promotion in the Process Industries (2001), 909–916.